NTNU

Norwegian University of
Science and Technology

Installation of subsea equipment – design and planning with focus on operability and weather windows

Ragnhild Brekke

PROJECT THESIS

Submission date: December 16th 2016

Supervisor: Professor Kjell Larsen

Norwegian University of Science and Technology

Department of Marine Technology

NTNU Trondheim
Norges teknisk-naturvitenskapelige universitet
Institutt for marin teknikk

PROJECT WORK AUTUMN 2016

for

Stud. tech. Ragnhild Brekke

Installation of subsea equipment – design and planning with focus on operability and weather windows

Installasjon av undervannsutstyr– design og planlegging med fokus på operabilitet og værventing

Background

In order to be able to design, install and operate a subsea oil and gas factory, a cost-effective and safe installation process is crucial. Present capital expenditure of the marine operations for a subsea production system in 300-500m water depth is for some cases in the range 20-30% of the total capital invested.

The main challenges with installation of subsea equipment are :
- Plan and perform installation operations more cost-effectively while maintaining safety and accuracy. This requires that the operations must be done smarter and faster using new methods and equipment. Increased use of autonomy is probably necessary. Included are also increased quality; the sub operations must be performed safely within a reliable weather forecast.
- Increase operational limits in order to extend the season where installation activities can be performed.
- Understand and manage the risk involved in the installation operation. An important part of this is to maximize the operability and to reduce the time for waiting-on-weather.
- Develop smarter and more time-efficient installation methods.

Scope of Work

1) Review relevant literature and describe state-of-art subsea installation methods by using crane vessels. A brief description of the technical challenges of the different phases from the lowering phase from the deck until accurately landed on the seafloor.
2) Describe how operability and time for "waiting-on-weather" can be quantified during the planning process of a marine operation. Some examples using weather data from Haltenbanken shall be made.
3) Estimate hydrodynamic coefficients in different phases of the lift of a pipeline installation cover. This cover shall be used in the subsequent MSc thesis. A check of the lifting wire tension loads shall be performed using the simplified method proposed in DNV-RP-H103. Relevant data for the cover will be provided by supervisor.
4) Conclusions and recommendations for further work.

General information

The work scope may change or prove to be larger than initially anticipated. Subject to approval from the supervisor, topics may be changed or reduced in extent.
In the project the candidate shall present her personal contribution to the resolution of problems within the scope of work.
Theories and conclusions should be based on mathematical derivations and/or logic reasoning identifying the various steps in the deduction.
The candidates should utilise the existing possibilities for obtaining relevant literature.

Report/Delivery
The project report should be organised in a rational manner to give a clear exposition of results, assessments, and conclusions. The text should be brief and to the point, with a clear language. Telegraphic language should be avoided.
The report shall be written in English and edited as a research report including literature survey, description of relevant mathematical models together with numerical simulation results, discussion, conclusions and proposal for further work. List of symbols and acronyms, references and (optional) appendices shall also be included. All figures, tables and equations shall be numerated.
The original contribution of the candidate and material taken from other sources shall be clearly defined. Work from other sources shall be properly referenced using an acknowledged referencing system.

The report shall be submitted in two copies:
- Signed by the candidate
- The text defining the scope included
- In bound volume(s)
- Drawings and/or computer prints which cannot be bound should be organised in a separate folder.

Ownership
NTNU has according to the present rules the ownership of the project results. Any use of the project results has to be approved by NTNU (or external partner when this applies). The department has the right to use the results as if the work was carried out by a NTNU employee, if nothing else has been agreed in advance.

Thesis supervisor**:**
Prof. II Kjell Larsen, NTNU/Statoil

Deadline: December 16th, 2016

Trondheim, December 8th, 2016

Kjell Larsen (date and signature):

Ragnhild Brekke (date and signature):

Preface

This paper is a Project Thesis about the topic *subsea lifting operations*. This is a part of my Master of Science degree in Marine Subsea Engineering at the Department of Marine Technology (IMT) at the Norwegian University of Science and Technology (NTNU) in Trondheim, Norway. The work has been carried out at NTNU during the autumn semester of 2016, in cooperation with Professor Kjell Larsen. The workload corresponds to 7.5 ECTS. The idea of the project was provided by Kjell Larsen, who works both at Statoil and as a professor at NTNU.

It is assumed that the reader is familiar with basic concepts of subsea lifting operations and hydrodynamics in general.

Trondheim, December 16, 2016

Ragnhild Brekke

Acknowledgements

First, I would like to thank my supervisor Professor Kjell Larsen for answering questions, providing information and recommendations for further work and giving guidance throughout the work on this thesis. He has made it easier for me to accomplish the aims with this paper.

I would also like to thank Statoil for providing input data to the operational planning case as part of this paper.

Norwegian Society Of Lifting Technology should be acknowledged for their generosity offering me a place at their Subsea Lifting Operations Seminar in Stavanger December 6^{th}-7^{th}.

Executive Summary

The environment has become more challenging the past years and marine operations must be performed in a smarter and faster way. Thus, design and planning of marine operations will be of high importance. A marine operation shall be designed to bring an object from one safe condition to another one and shall be performed within defined safety levels and planned according to defined rules and standards.

A pipeline GRP cover installation is defined as a weather restricted level B marine operation, and shall be carried out at Heidrun and Tanzania Block 2. The planned operation's reference period is determined to be 12 hours. To be able to account for uncertainty in weather forecast, the operation design criteria will be reduced by an α-factor. The operational criterion is the maximum weather condition for execution of the marine operation and is determined during the planning process. Calms are periods where the significant wave height is less than the operational criteria. The operation can only take place when the weather forecast predicts a calm period with a length greater than the determined reference period.

Weather conditions are season dependent and affect and delay marine operations. High operability and short time for waiting-on-weather is desired at all time. Observed length of calms during each season were calculated at both Heidrun and Tanzania. For a design criterion of 2 m, average operability at Heidrun varied between 63.2% during summer and 24.3% during autumn. At Tanzania average operability varied between 91.1% during summer and 84.6% during winter. At both fields the operability increased with approximately 25% when the design criterion was increased to 3 m.

A subsea lift consists of different phases that should be evaluated during the planning process. Two lifting scenarios for the pipeline GRP cover were investigated; vertical and horizontal rigging. The appurtenant phases were considered separately and the hydrodynamic parameters and resulting force were calculated by use of the Simplified Method. The aim with this method is to achieve simple conservative estimates of the forces acting on the cover during different phases. Added mass and drag forces are important hydrodynamic parameters that depend on the projected area of the submerged part of the cover. Thus, the resulting force was found to be highly dependent on the rigging scenario.

The relation between the added mass and the projected area is non-linear, thus the total added mass value differentiated depending on how the projected area was divided. Two techniques were investigated; the Superposition-Technique and the Plate-Technique. Added mass found by use of the Plate-Technique was significantly larger than for the Superposition-Technique. For both vertical and horizontal rigging larger forces acted on the system when the cover was lifted through the splash zone. The total resulting force acting during a vertical lift was considerably lower than for a horizontal lift. The hoisting wire material and dimensions should be determined based on the system natural frequency in such a way that resonance is avoided.

Contents

List of Tables

List of Figures

1 Introduction

1.1 Background

The environment has become more challenging the past years and exploration of new frontiers is becoming more common. With this follows many challenges that have to be solved in an cost-effective and safe way. Thus, design and planning of marine operations will be of high importance. Present capital expenditure of the marine operations for a subsea production system in 300-500m water depth is for some cases in the range 20-30% of the total capital invested.

Marine operations must be performed in a smarter and faster way by introducing new installation methods and equipment. An increase of operational limits in order to extend the season where the operational actions can take place should be performed. By getting familiar with the different lifting phases and which challenges and risks that may occur, operations can be carried out in a safe, effective and smart way. Deep water operations introduce new challenges and will confront already existent rules and standards.

A pipeline GRP cover installation shall be performed at Heidrun and Tanzania Block 2. GRP covers have been installed offshore for many years, and is a part of general installation procedures. However, few analysis and calculations of hydrodynamic forces acting on the cover during a lift have been performed.

1.2 Objectives

As stated in the enclosed work description, the objectives of this thesis can be summarised as followed:

1. Review relevant literature and describe state-of-art subsea installation methods by using crane vessels. A brief description of the technical challenges of the different phases from the lowering phase from the deck until accurately landed on the seafloor.

2. Describe how operability and time for “waiting-on-weather” can be quantified during the planning process of a marine operation. Some examples using weather data from Haltenbanken shall be made.

3. Estimate hydrodynamic coefficients in different phases of the lift of a pipeline installation cover. This cover shall be used in the subsequent MSc thesis. A check of the lifting wire tension loads shall be performed using the simplified method proposed in DNV-RP-H103. Relevant data for the cover will be provided by supervisor.

4. Conclusions and recommendations for further work.

1.3 Structure of the paper

The rest of the paper is organised as followed:

- Section 2 presents assumptions that have been made to be able to conduct appropriate hand calculations in an efficient way.
- Section 3 gives general information about marine operations, operational criteria, weather windows, key challenges with marine operations and recommended steps during a planning process.
- Section 4 presents the different lifting phases and categorises typical lifts.
- Section 5 presents the input data that is used in this paper, where cover dimensions and data sets, containing observed environmental conditions at Heidrun and Tanzania, are designated.
- Section 6 provides operational criteria for the installation and visualises how the installation is divided into different lifting phases.
- Section 7 gives the results for the installation operability at Heidrun and Tanzania.
- Section 8 presents the hydrodynamic methodology and describes how the tension in the hoisting wire can be calculated and how hydrodynamic parameters can be determined by use of the Simplified Method.
- Section 9 gives all the established hydrodynamic parameters during various lifting phases.
- Section 10 gives the resulting forces calculated by the Simplified Method during various lifting phases.
- Section 11 provides a discussion, synthesising on the aforementioned material, the proposed framework and error sources.
- Section 12 presents the conclusions of the thesis and recommendations for further work.

2 Assumptions

Some assumptions have been made to be able to conduct appropriate hand calculations in an efficient way.

The rigging equipment used to lift the pipeline GRP cover was not included when the resulting force was calculated. Currents and wind were not taken into account during the planning of the operation.

By assuming a horizontal sea bottom and a free-surface of infinite horizontal extent, linear wave theory could be used for the propagating waves (Faltinsen, 1990). It was also assumed that the pressure followed Bernoulli's equation, infinite water depth and that the sea was incompressible, inviscid and that the fluid motion was irrotational.

DNV GL's α-factors, found in appendix A.1, were used for both the Norwegian and Tanzanian fields. The α-factors were based on the assumptions of no seasonal nor area variations, no differences between the providers and that the forecasts were according to Normal Distribution (Lundby, 2006).

Heave, pitch and roll Response Amplitude Operators (RAOs) for the vessel were not considered when the vertical motion of the crane tip was determined.

It was assumed that the crane tip and water particle velocity were time-independent, and that the crane tip was located 30m above sea surface.

Increase of added mass as the lifted object approaches the sea bottom was neglected.

3 Marine Operations

A marine operation is a non-routine operation of a limited defined duration related to handling objects and/or vessels in the marine environment. A marine operation shall be planned and performed with adequate consideration for environmental conditions and vessel motions' and structural loads' operational limits (Natskår et al., 2015). A marine operation shall be designed to bring an object from one defined safe condition to another safe condition. A safe condition is where the object is considered exposed to *normal* risk for damage or loss, where *normal* refers to a risk similar to the risk expected during *in-place* condition. Marine operations shall be performed within defined safety levels, and the design acceptance criterion is to ensure a probability for structural failure less than 10^{-4} per operation (Larsen, 2016). The given probability might increase when operational errors, human errors and other factors that affect the probability are taken into account.

A marine operation shall be planned according to defined codes and standards to ensure high safety. The operations should be designed based on the assumption that it may be needed to interrupt by either reversing the operation or bring it back to a safe condition.

Marine operations are divided into two categories; weather restricted and weather unrestricted operations. A weather restricted operation shall be of a limited duration, and the planned operation time is usually less than 72 hours. The operation can take place safely within the limits of a given weather forecast. A weather unrestricted operation can take place safely in any weather condition and is usually longer than 72 hours. The weather window for an unrestricted operation is based on long term statistics with seasonal and statistical extremes for the operation area. The weather window for a restricted operation is given by forecasts at the wanted operation location, independently of statistical data. Thus, the operation can be designed and planned for a significantly lower environmental condition than an unrestricted operation. A consequence of planning a weather restricted operation is that an α-factor has to be considered. The α-factor takes uncertainties in the weather forecast into account. This is further described in *section 3.1 The α-factor*. Maximum wave height H_{max} for a weather restricted operations is $2 \cdot Hs$ (DNV GL, 2011a).

A marine operation's reference period T_R is given by equation (3.1) and is the total operation period. T_{POP} is the planned operation period and starts simultaneously when the first weather forecast is given. T_C is the estimated maximum contingency period.

$$T_R = T_{POP} + T_C \tag{3.1}$$

T_{POP} should be based on a detailed, planned schedule for the operation and is the basis for selecting the α-factor. T_C shall consider uncertainties in the planned operation period and for a weather restricted operation T_C shall cover possible unforeseen situations and delays due to weather (DNV GL, 2011a). The relation between T_{POP}, T_C and T_R is shown in figure 3.1.

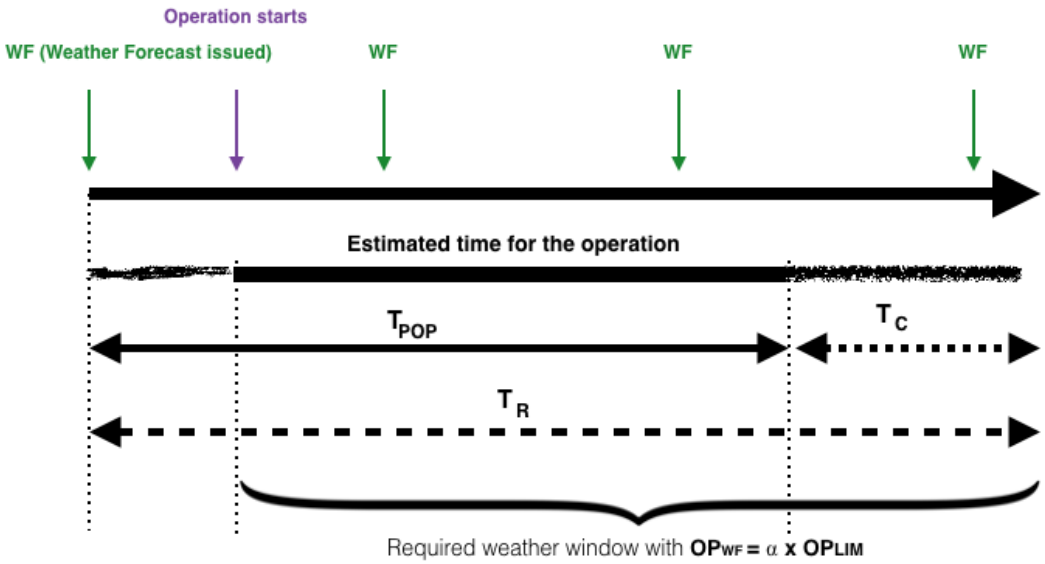

Figure 3.1: Weather Window

Weather restricted marine operations are divided into three categories; level A, B and C. Every category has its own requirements that have to be fulfilled before the operation can take place. These requirements can be found in table 3.1. Level A marine operations are major operations sensitive to weather, such as mating operations, offshore float over and offshore installation operations among others. Level B marine operations are of significant importance with regard to value and consequences, and are sensitive to weather conditions. Such operations can be offshore lifting and subsea installation. Level C marine operations are more ordinary operations less sensitive to environmental conditions, such as onshore and inshore lifting.

Table 3.1: Weather Forecast Levels (DNV GL, 2011a, H101, section 4)

Weather Forecast Level	Meteorologist required on site?	Independent WF WF sources	Maximum WF interval
A	Yes[1]	2[2]	12 hours[3]
B	No[4]	2[5]	12 hours
C	No	1	12 hours

[1] There should be a dedicated meteorologist, but it may be acceptable that he/she is not physically present at site. The meteorologist opinion regarding his/her preferable location should be duly considered. It is anyhow mandatory that the dedicated meteorologist has continuous access to weather information from the site and that he/she is familiar with any local phenomenon that may influence the weather conditions. Note also that the meteorologist shall be on site in order to use alpha factors from table A.2 and A.3 in appendix A.1.

[2] It is assumed that the dedicated meteorologist (and other involved key personnel) will consider weather information/forecasts from several (all available) sources.

[3] Based on sensitivity with regards to weather conditions smaller intervals may be required.

[4] Meteorologist shall be conferred if the weather situation is unstable and/or close to the defined limit.

[5] The most severe weather forecast to be used.

3.1 The α-factor

To be able to account for uncertainties in weather forecasts, the weather limit for execution of a marine operation has to be reduced compared to the design weather conditions. This is done by introducing an α-factor. The α-factor is based on T_{POP} and Hs and is a good correlation between forecasted and observed values, within Europe (Lundby, 2006). It is an important parameter for safety and cost of offshore operations. It should be as reliable as possible to be able to maintain high operation operability. A complex marine operations should be divided into sub operations for which different α-factor can be determined. The α-factor is the relation between the design criterion and the operational criterion, and is given by equation (3.2). The design criterion OP_{LIM} is the weather condition used for calculation of design load effects. OP_{LIM} should never be taken greater than; maximum environmental criteria, the conditions for safe working of personnel, the equipment restrictions or limiting conditions for diving systems and position keeping (Alvær, 2008). The operational criterion OP_{WF} is the maximum weather condition for execution of the marine operation and is determined during the planning process and controlled by the weather forecast (Larsen, 2016).

$$OP_{WF} = \alpha \cdot OP_{LIM} \tag{3.2}$$

The α-factor has a magnitude less than one and will increase with increased quality of weather forecasts and the use of on-site monitoring systems. It decreases with the planned length of the operation, hence the difference between OP_{LIM} and OP_{WF} increases with increased T_{POP}.

The α-factor should be estimated based on the weather uncertainty for the actual site and the planned period of the operation. It includes the fact that it is harder to estimate the wave height for small sea conditions than for larger seas. The α-factor should be calibrated to ensure that the probability of exceeding the design criterion with more than 50% is less than 10^{-4} (DNV GL, 2011a). Hs is a preferred assessment parameter because waves are considered as the most influencing parameter, with respect to performance, for the majority of marine operations. The amount, availability and quality of the data records for Hs are usually satisfactory (DNV, 2007).

The α-factor was introduced in 1995 as an allowance for uncertainties in forecasted versus actual weather. It was based on forecasted and observed values over a period of two years at two locations in the North Sea and *one* provider. When introduced it was considered a more accurate and documented approach than all previous practice. The α-factor found in 1995 did not consider short term operations with real time monitoring of environmental conditions. One of the main challenges in 1995 was a limited amount of data available (DNV, 2007). The α-factor was improved in 2006 due to increased quality of forecasting services and more advanced monitoring techniques. The update was based on more locations and *three* providers (Alvær, 2008). Some consistent improvements from the 1995 results were found, but these were less than initially expected (DNV, 2007). α-factors for different marine operation levels can be found in *appendix A.1*.

3.2 Weather Window

A weather window is a period of time which is sufficient in length to safely carry out a marine operation. Weather forecasted environmental conditions shall remain below the Operational Criterion (OP_{WF}) for the whole length of the period (Larsen, 2016). Figure 3.2 and 3.3 show examples of observed length of calms with significant wave height at Heidrun and Tanzania respectively. HS_{WF} and T_R were determined to be 3 m and 72 hours respectively, and the criteria segregate the observed length of calms into *work*- and *wait*-categories.

A calm period is a period where Hs is lower than the operational criterion and is called *calms* (τ_C), while a storm period is a period where Hs is higher than the operational criterion and is called *storms* (τ_S). One is only allowed to operate when the weather forecast predicts a calm period that is of *longer* duration than the determined reference period T_R.

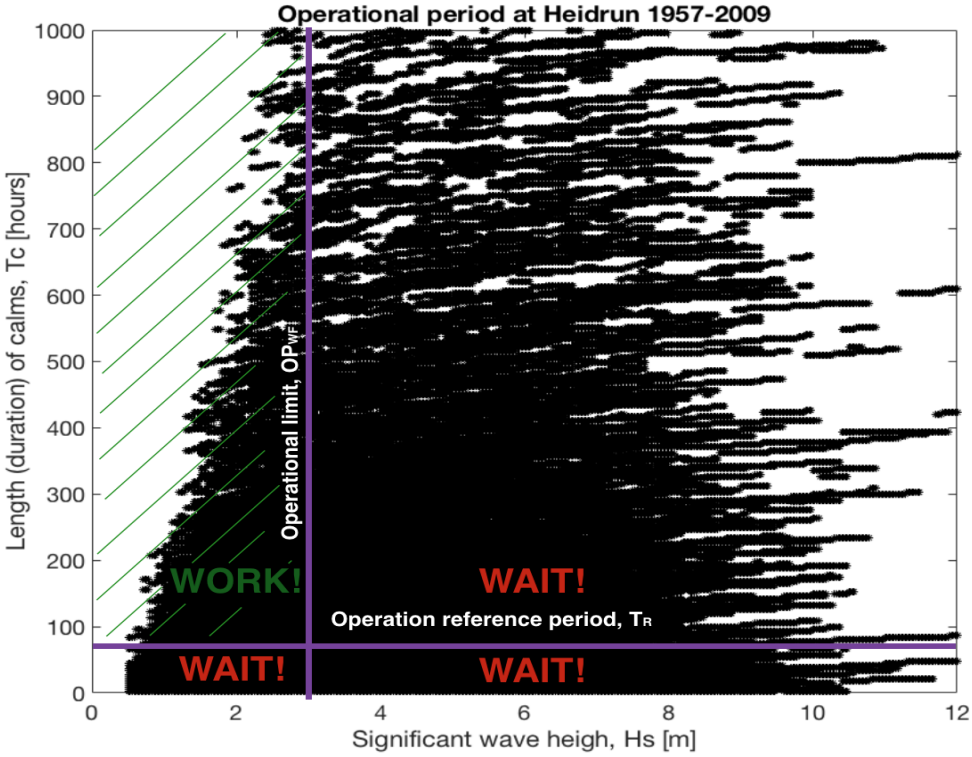

Figure 3.2: Observed length of calms for different Hs_{WF} at Heidrun.

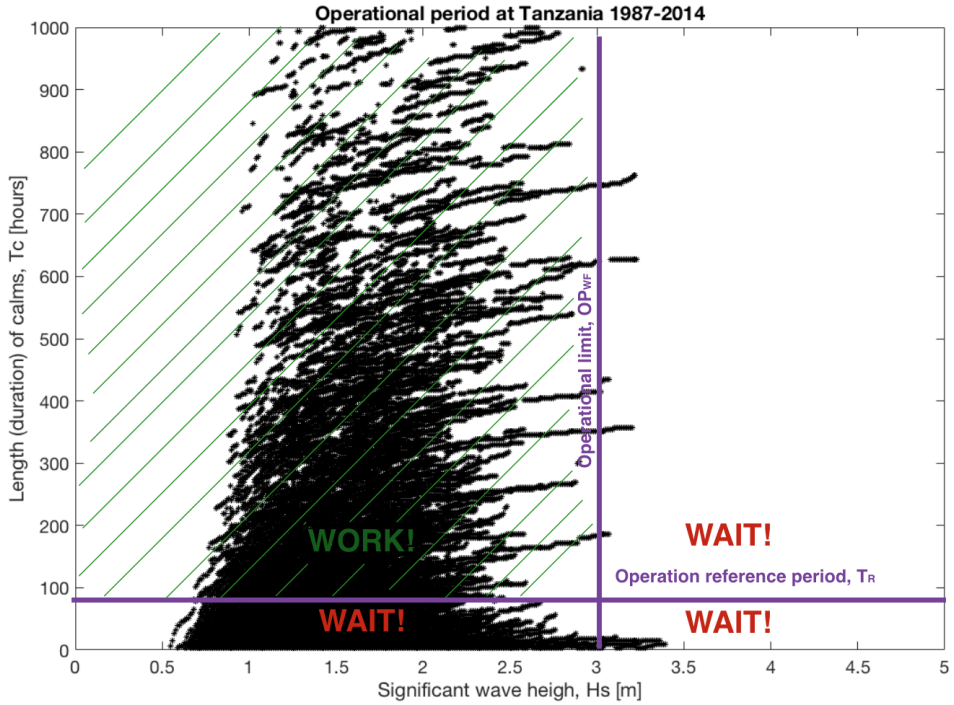

Figure 3.3: Observed length of calms for different Hs_{WF} at Tanzania.

Figure 3.4 shows how significant wave height varies at Heidrun during 1958, with examples of calms and storms, work and wait periods. The operational Hs-criterion was set to 2 m.

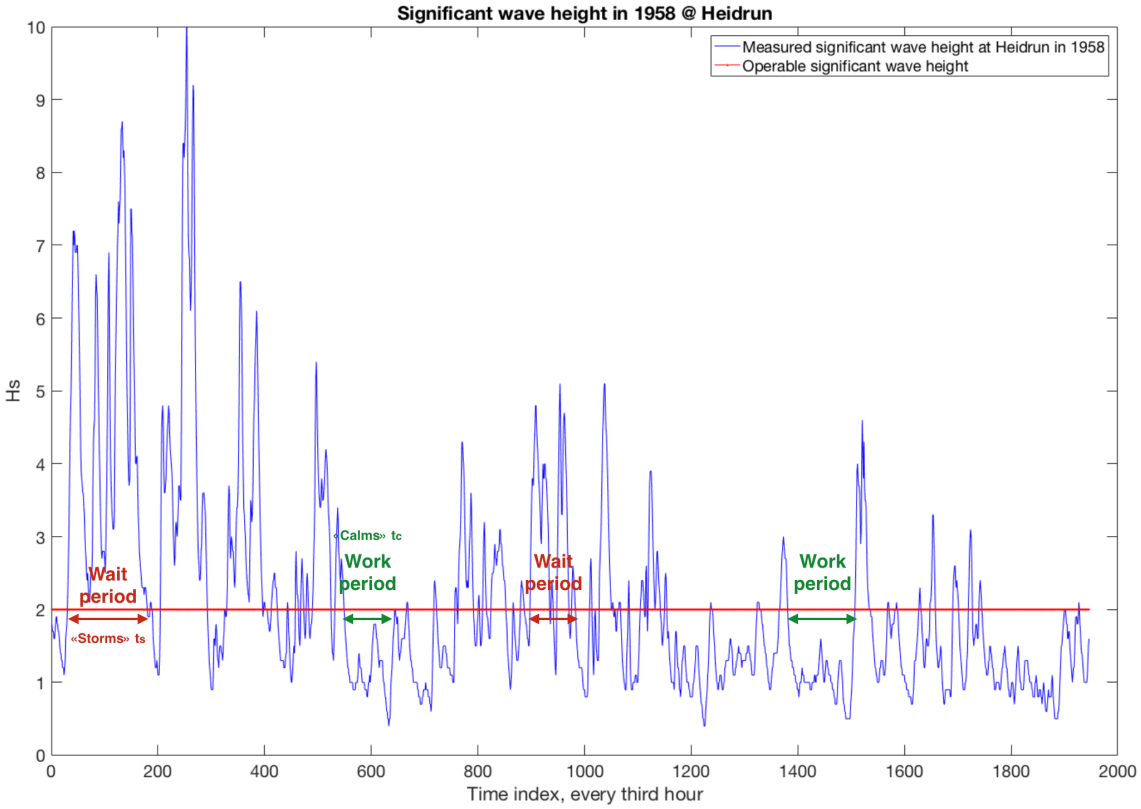

Figure 3.4: Significant wave height at Heidrun in 1957.

3.3 Probability Distributions

It is often interesting to know the probability density distribution of observed data, in such a way that it can be used to predict future outcomes. The *Weibull distribution* is one of the most common used distributions in reliability engineering. The distribution is usually based on *two* parameters; scale (γ)- and shape (β) parameter. Different combinations of the parameters can result in several other distributions. The shape parameter is a numerical parameter of a parametric family of probability distributions (ReliaWiki, 2016). If 0 < β < 1, the distribution has a decreasing failure rate over time. If β = 1, the distribution is identical to an exponential distribution with constant failure rate. If 1 < β < 2, the distribution has an increasing failure rate over time. Cumulative probability of length of calms τ_c is described by a Weibull distribution as in equation (3.3) (van Voorthuysen, 2015).

$$F(t) = 1 - exp(-\Big(\frac{\tau_c}{\gamma}\Big)^{\beta}) \tag{3.3}$$

The probability of being able to work can be determined by equation (3.4) (Larsen, 2016).

$$P\Big((Hs \leq OP_{WF}) \cap (\tau_c \geq T_R)\Big) = \sum_{Hs=0}^{Hs=OP_{WF}} P\Big((\tau_c \geq T_R)|Hs\Big) \cdot P(Hs) \tag{3.4}$$

3.4 Key Challenges

The environment has become more challenging the past years and exploration of new frontiers and areas is more common. Some challenges are deep water oil and gas operations in up to 3000 meters depth, operations in arctic areas and operations related to renewable energy such as offshore wind. The aquaculture is becoming more competence driven and more strict regulations have been developed also within this area. The combination of environmental conditions as wind, waves and current are hard to simulate and achievement of adequate results are difficult. During a deep water lift, the static weight on the crane tip will increase due to a longer hoisting wire. This might lead to larger oscillation periods in heave and a decreased cable stiffness. The drag forces in horizontal direction may increase due to the cable's large projected area, and large offset may occur. It is difficult to manoeuvre and relocate an object in deep water, which can provide operation delays (Larsen, 2016).

To increase the lifetime of already existing structures and equipment, complex maintenance and reparations have to be performed. Removal of marine structures might be challenging and involve new vessel types. More complex operations and larger modules may introduce difficulties in simulations. There are strict requirements to cost, efficiency and safety, and to optimise the operation based on these three requirements, detailed planning and design become highly important. To ensure safety it is important to understand and manage exposed risk and system behaviour. Increased weather windows will optimise operation cost and efficiency. Typical marine operation risks are position loss, collisions and grounding during transport, icing, dropped objects and structural failures.

Also lack of competence of personal and insufficient operational procedures are of potential high risk (Larsen, 2016).

Planning and performing installation operations more cost-effectively while maintaining safety and accuracy will always be a challenge. Smarter and faster solutions are required, and increased use of autonomy is probably necessary. Political requirements, e.g. emission regulations, introduce new challenges in terms of cost, efficiency and safety and may result in development of new technology.

3.5 The Planning Process

Planning of a marine operation shall be according to *fail safe*-principles. An operation is safe if it fails to a safe state (Gjersvik, 2015). Planning is important to ensure safety and reduce cost. The operation's classification in terms of weather restrictions might have a great impact on the safety and the cost of the operation. Thus, it should be defined as early as possible in the planning process. The planning should as far as it is attainable be based on well proven principles, techniques, systems and equipment. Operations within an unknown environment or with new technology shall be documented through acceptable qualification processes. During the planning process any unforeseen situations shall be identified, and plans or actions shall be made to prevent those kinds of situations. When a marine operation shall be planned and designed, DNV GL recommends to follow the iterative procedure in figure 3.5.

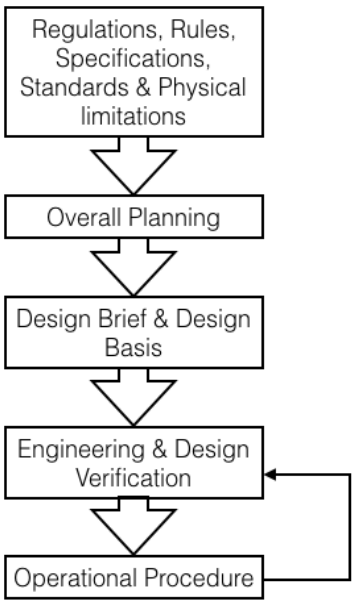

Figure 3.5: DNV GL's recommened planning procedure (DNV GL, 2011a)

The following sequence includes more details for each step in figure 3.5 (DNV GL, 2011a, H101, section 2).

1. Identify rules, company specifications and standards and physical limitations as surveys of structures and local environmental conditions
2. Overall planning; operational concepts, available vessels and equipment, cost and schedule and risk assessment
3. Establish design basis and briefs; describing environmental conditions and physical limitations, and specify applicable codes and acceptance criteria
4. Perform design; estimate load effects and decide required structural resistance
5. Develop operation procedures

To ensure planning with appropriate safety margins and weather forecast all marine operations shall be documented. The documentation shall be checked by an external part before the operation takes place. The documentation shall include environmental conditions, criteria and weather forecasts (Larsen, 2016).

4 Lifting Procedures

4.1 Lifting Phases

A subsea lift consists of different phases; lift off and in air, lowering through splash zone, further lowering to seabed and positioning and landing. All the phases shall be evaluated during the planning process. The following subsection will describe the different phases in detail, in addition to highlight the challenges that one can be exposed for during each phase.

4.1.1 Lift Off and In Air

A lift off operation includes lift from other vessel, from deck or from shore. In this paper a lift off is referred to as lifting from deck of a crane vessel. Before the lifting can take place, the sea fastening has to be undone. If the weather restrictions allow it, this process can start prior to the given planned operation period, while waiting on operational weather window. The duration of this process is highly dependent on how it is sea fastened, e.g. if it is strapped or welded.

Vertical and horizontal motions of the crane tip will occur when the crane starts to lift. Dynamic coupling between the object and the vessel arise occur. Ballasting operations might be performed to compensate for these motions, either by active ballasting or anti-heeling systems. It is important to be aware of the crane radius and its reach capacity. For safety reasons it is important to ensure clearance to other structures and people, and have clear communication between deck crew, crane operator and the bridge.

Identified hazards during lift off can be unacceptable tension in lifting wire and horizontal motion or re-hit of object after lift off. It is important to be aware of the criteria related to these hazards, and determine the hoisting speed based on the wire stiffness, mass of lifted object with rigging equipment and other forces acting on the lifting system.

In air, when the crane rotates and lift the object over the vessel rail, wind and other weather conditions and limitations are of great importance. Manoeuvring the object may be difficult, so tugger lines can be used to guide the object through the splash zone. One must be aware of the limitations of all equipment used in the lift off- and in air phase, and snap loads have to be avoided (Larsen, 2016).

4.1.2 Splash Zone

The splash zone is the part of the installation where the structure is intermittently exposed to air and immersed in the sea (DNV GL, 2008). During this phase following forces will act on the lifted object; force in hoisting wire, weight of object in air, buoyancy, current, inertia, wave damping, drag, wave excitation, slamming and water exit force - making this phase the most critical one. The forces have to be taken into account when total response is going be determined. Some of these forces are difficult to predict and calculate, hence a simplified method for estimating the hydrodynamic forces will be introduced (DNV GL, 2011a). This method is further described in *section 8.5 Simplified Method*.

Lifting through the splash zone might introduce snap loads due to slack in lifting lines. Snap loads are impact loads caused by abrupt retensioning of the line, which occurs if the cable system is exposed to motions with large amplitudes and/or high frequency. Slack occurs in the line when the decrease in dynamic tension exceeds the static load, hence snap loads arise (NTIS, 1973). To prevent snap loads and to be able to manoeuvre the object easily through the splash zone, module handling systems can be used.

The lifted object might be exposed to instability due to unsymmetrical submergence or filling. This can lead to unsymmetrical forces in the lifting wires and in worst case result in exceeding the designed criteria. Rotation of the object might also occur, and without awareness this can lead to complications in subsequent phases.

4.1.3 Lowering

During further lowering of the object the water depth and the cable length will increase. A complex structure might have air trapped inside it that has to be released. Defined wait period has to be included in the plan. Light structures usually have a slow sinking speed that has to be considered (Brandsvoll, 2016).

Cable stretch can occur due to cable weight and weight of lifted object. Ocean current can be time-dependent and vary with depth. Strong currents can lead to horizontal offset of the lifted object. Increased horizontal drag forces can be observed due to larger projected area with increased cable length. Wave induced motion of the vessel crane tip can lead to vertical oscillations of the lifted object, which can, in some cases, result in dynamic resonance. Heave compensation, which is a system that can compensate for an object's heave motion, can be used to control the vertical motion (Larsen, 2016).

4.1.4 Landing on Seabed

Landing of the lifted object must take place in exact location and in designated rotation. The positioning of the object can be performed by an ROV holding onto a pram handle, by positioning the vessel or by use of clump weights and a distance wire (Brandsvoll, 2016). Accurately and efficiently the ROV will relocate the object. Repositioning of the vessel is a time consuming process and it is not given that it will result in wanted outcome. Using distance wires and clump weights are a known and reliable process, but is also time consuming. By introducing new technologies, thrusters can be attached to the object and steered from the vessel.

The landing speed of the lifted object is important. Constant tension in the wire is desired and as for lift off, one has to be careful with possible re-hit. Slight differences in seabed characteristics will induce tilt on the object (Brandsvoll, 2016).

4.2 Heavy- and Light Lifts

It is important to be aware of the objects weight while planning a lifting operation. The ratio between the weight of the lifted object and the vessel classifies the lift. If the object's weight is less than 1-2% of the vessel's weight it is classified as a *light lift*. If the object's weight is above 1-2% of the vessel's weight it is classified as a *heavy lift*. During a light lift operation, the lift will not affect the vessel's motion. Heave compensation can be used during a light lift operation. During a heavy lift operation, there will be dynamic coupling between the lifted object and the vessel, in addition to hydrodynamic coupling from the environment. This leads to a more complex operation and heave compensation cannot be used. A heavy lift is usually above a thousand tonnes (Larsen, 2016).

4.3 Heave Compensation

Heave compensation is one method of controlling the vertical motion of a lifted object and control the tension in the lifting wire during a lifting operation. Using heave compensation the weather window, the safety and efficiency can be increased. Vertical motion is a combination of the vessel's heave motion and rolling moment. There are two main heave compensator groups; Passive Heave Compensation (PHC) and Active Heave Compensation (AHC). A passive heave compensator is a spring/damper system that does not consume external power. PHC is effective for shock absorption through the splash zone phase, and can also be effective in eliminating any resonance that can occur. An active heave compensator does utilise external power. AHC actively control the wire length to compensate for the vertical motion. It is an accurate, but time consuming technique, and is effective during landing on seabed (Larsen, 2016).

5 Input Data

5.1 Pipeline GRP Cover

The subsea pipeline cover that is going to be installed is made of Glass-Reinforced Plastic (GRP) and is shown in figure 5.1 and has mass dimensions as described in table 5.1.

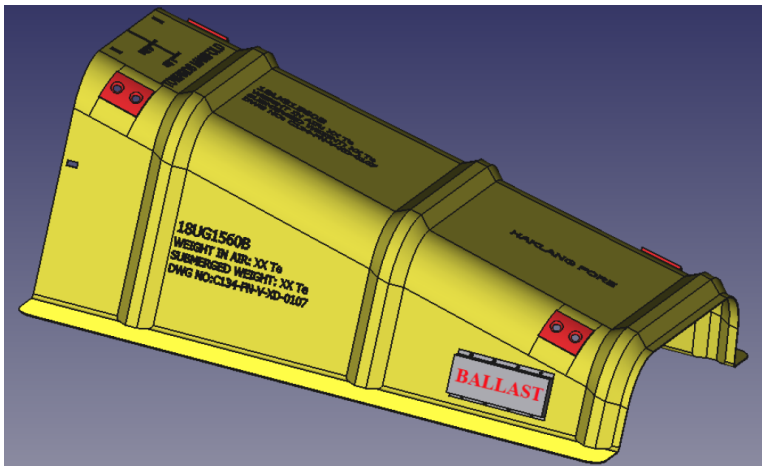

Figure 5.1: CAD model of GRP cover (Tharigoupla, 2016)

Table 5.1: Mass of Cover (Kendon, 2016)

	Mass	Density	Volume
Cover	7 144 kg	1 940 kg/m^3	3.682 m^3
Ballast	4 756 kg	7 866 kg/m^3	0.605 m^3
Total	**11 900 kg**		**4.287 m^3**

The true dimensions of the cover are shown in figure 5.2, including centre of gravity (*COG*) for the cover in air and submerged. COG for the cover is calculated to be 1.425 m and 1.297 m from underneath the flaps and 6.914 m and 7.303 m from the biggest opening - in air and for a submerged condition respectively.

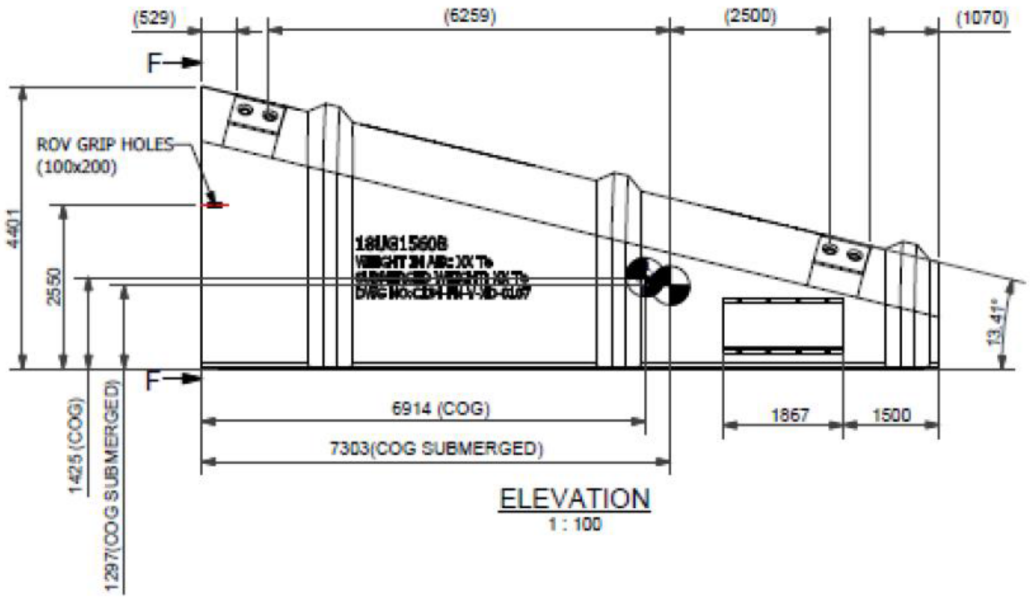

Figure 5.2: Cover dimensions with COG (Statoil, 2015)

To be able to do efficient and adequate hand calculations, the cover shape is simplified to have dimensions as shown in figure 5.3.

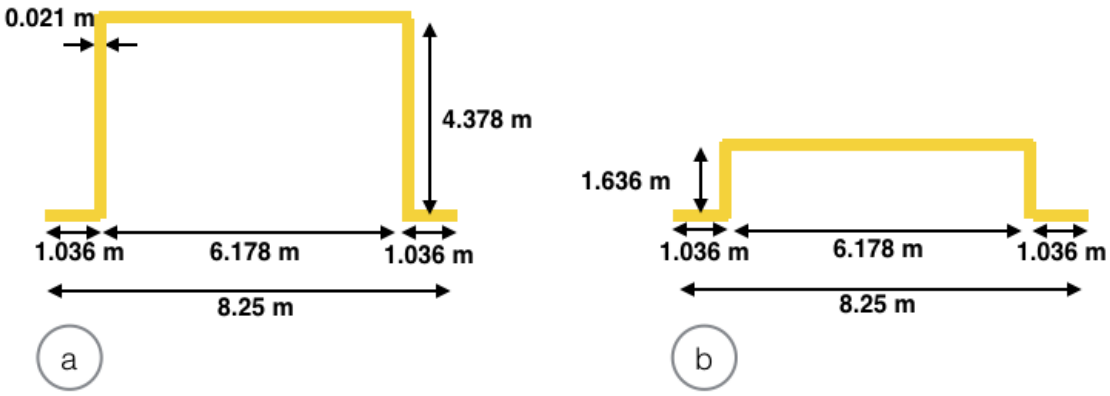

Figure 5.3: Dimensions of simplified GRP-cover, (a) front and (b) back

5.2 Environmental Conditions

The installation of the GRP-cover operation shall take place at two locations; Heidrun and Tanzania Block 2. The Heidrun oil and gas field is located at Haltenbanken, west off the Norwegian coastline. Tanzania Block 2, hereinafter referred to as Tanzania, is located off the coast of Tanzania east in Africa. The locations are shown on two maps in figure 5.4 and 5.5, for Tanzania and Heidrun respectively.

Figure 5.4: Location of the Tanzania field

Figure 5.5: Location of the Heidrun field

Local environmental conditions have been observed and stored every three hours for 52 years and 27 years at the Heidrun and Tanzania respectively. The geographical coordinates for the two fields and the start and end date for the data sets are listed in table 5.2. The water depths at Heidrun and Tanzania are approximately 350 m and 2460 m respectively. Information about the data sets is found in Statoil's Metocean reports for Heidrun (Eik and Nygaard, 2004) and Tanzania (Mathiesen, 2010).

Table 5.2: Time Series Information

Field	Latitude	Longitude	Start date	End date
Heidrun	65.29N	7.32E	01.01.1958	31.12.2009
Tanzania	9.25S	40.38E	01.01.1987	31.12.2013

The data sets are divided into seasons. Norway and Tanzania are located on the opposite side of equator resulting in opposite seasons. In Norway, planned operations usually take place during late spring, summer, and early autumn. Late spring and early autumn will hereinafter be referred to as spring and autumn respectively, while the rest of the months will be referred to as *off-season*. In Tanzania the different seasons will contain the appurtenant three months. The correlation between months and seasons in Norway and Tanzania is shown in figure 5.6.

	January	February	March	April	May	June	July	August	September	October	November	December
Heidrun	Off-Season			Spring		Summer			Autumn		Off-Season	
Tanzania	Summer		Autumn			Winter			Spring			Summer

Figure 5.6: Correlation between months and seasons in Norway and Tanzania

6 Planning

6.1 Operational Criteria

There were three important parameters that had to be determined during the planning process of the marine operation; the reference period T_R, the design criterion OP_{LIM} and the $\alpha - factor$. All the planning phases had to be examined separately, before T_{POP} could be determined. T_C consider all uncertainties and T_R summarise the two periods.

It was assumed that the total duration of the lift off, in air and through splash zone phase had a duration of up to two hours. The planned operation period was dependent on water depth resulting in different planned operation periods at Heidrun and Tanzania. With an average launching speed of 0.3 m/s, the lowering phase was calculated to be approximately 20 minutes at Heidrun and up to two and a half hours at Tanzania.

The average current speed $u_{current}$ at Heidrun was approximately 0.113 m/s (Eik and Nygaard, 2004) throughout the water column, significantly weaker than at Tanzania where $u_{current}$ was approximately 0.254 m/s (Mathiesen, 2010). A possible offset would therefore have higher probability of occurrence at Tanzania than at Heidrun, thus relocation of the object had to be considered in T_{POP}.

T_{POP} at Heidrun was determined to be approximately 2 hours while at Tanzania T_{POP} was approximately 6 hours. If uncertainties in the planned operation period and required time for contingency situations was not assessed in detail, T_C should be similar to T_{POP} (DNV GL, 2011a). T_R was determined to be 4 hours at Heidrun and 12 hours at Tanzania.

Offshore lifting and installation of a pipeline GRP cover was determined to be a level B operation. If the available weather forecasting services could be regarded as level B, and the highest forecasted wave heights from at least two recognised and pre-defined sources were considered, the α-factor could be determined according to table 6.1 (DNV GL, 2011a).

Table 6.1: α-factor for waves, level B highest forecast (DNV GL, 2011a)

Operational Period	**Design Wave Height** [m]				
[hours]	$H_S = 1$	$H_S = 2$	$H_S = 3$	$H_S = 4$	$H_S = 6$
$T_{POP} \leq 12$	0.68	0.80	0.82	0.83	0.84
$T_{POP} \leq 24$	0.66	0.77	0.79	0.80	0.82
$T_{POP} \leq 36$	0.65	0.75	0.76	0.77	0.80
$T_{POP} \leq 48$	0.63	0.71	0.73	0.75	0.78
$T_{POP} \leq 72$	0.58	0.66	0.69	0.71	0.76

Both fields had a planned operation period less than 12 hours. Thus both fields had the same α-factor of 0.80 and 0.82 for a design wave height Hs_{LIM} of 2m and 3m respectively. The operational wave height Hs_{WF} was calculated to be 1.60 m and 2.46 m when Hs_{LIM} was 2m and 3m respectively.

6.2 Lifting scenarios

The pipeline GRP cover can be installed in several ways. Two lifting scenarios were investigated in this paper; vertical and horizontal rigging. The two scenarios are extremities with lifting angles of 90° and 0° respectively. The cover can be installed with any angle in between, and a vertical lift with an angle of 68° is shown in figure 6.1.

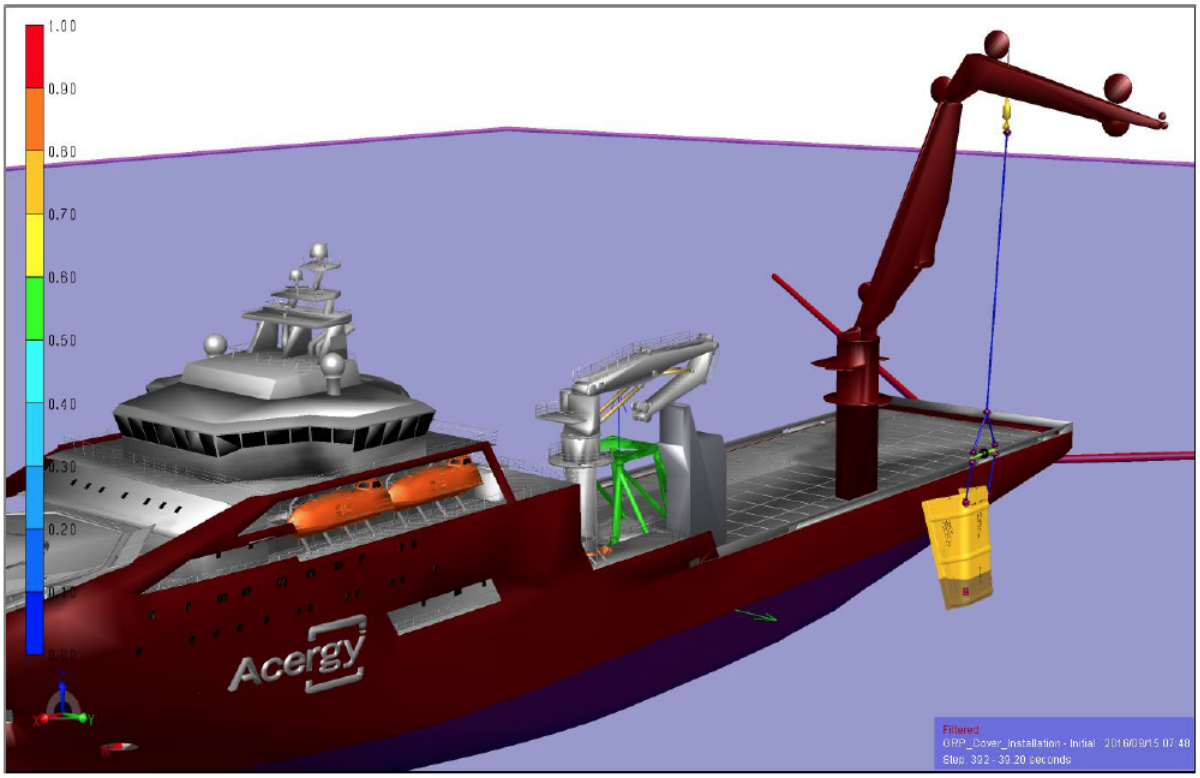

Figure 6.1: Vessel lifting GRP cover in vertical direction (Statoil, 2015)

Hydrodynamic parameters were calculated for the two different lift scenarios. Each lifting scenario contained three main lifting phases; In Air, Through Splash Zone and Fully Submerged.

6.2.1 Vertical Rigging

The three main lifting phases for a vertical rigging are shown in figure 6.2.

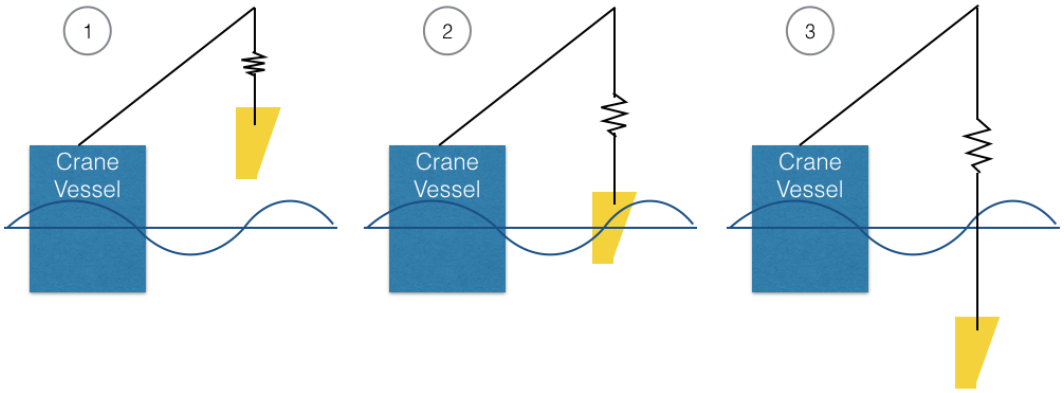

Figure 6.2: Vertical Rigging: 1. In Air, 2. Through Splash Zone, 3. Fully Submerged

The submerged depths of the cover during the different phases for a vertical lift, are shown in table 6.2. z is the distance from sea surface to the lower bound of the cover, and d is the distance from sea surface to the cover centre of gravity. The table does also include *half-phases (a) - half immersed and (b) - fully immersed* for phase 2 - Through Splash Zone. The half-phases are shown in figure 6.3.

No hydrodynamic forces will act on the object during the *in air*-phase

Table 6.2: Phases during a Vertical Lift

Vertical Rigging	z	d
1 - In Air	0 m	0 m
2 - Through Splash Zone		
(a) - half immersed	6.500 m	0.609 m
(b) - fully submerged	13.000 m	7.303 m
3 - Fully Submerged	23.000 m	17.303 m

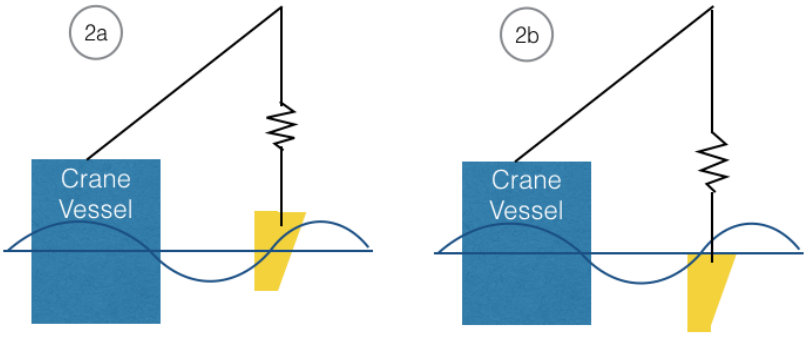

Figure 6.3: Lifting through splash zone: (a) - half immersed, (b) - fully immersed

6.2.2 Horizontal Rigging

The three main lifting phases for a horizontal rigging are shown in figure 6.4.

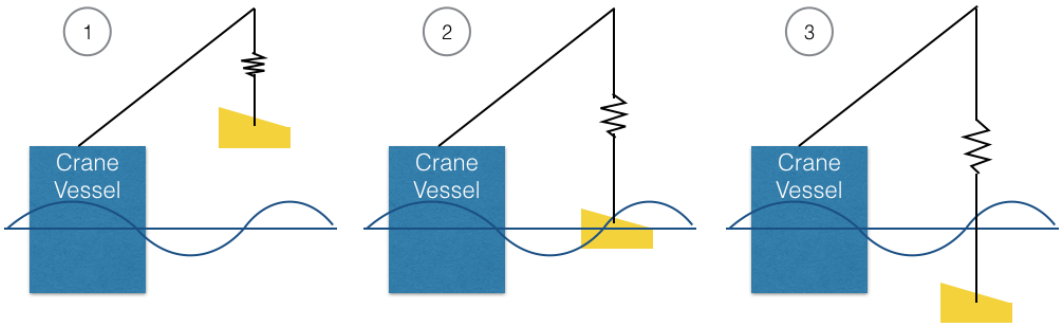

Figure 6.4: Horizontal Rigging: 1. In Air, 2. Through Splash Zone, 3. Fully Submerged

The submerged depths of the cover during the different phases for a horizontal lift, are shown in table 6.3. The table does also include *half-phases (a) - only flaps immersed, (b) - half immersed and (c) - fully immersed* for phase 2 - Through Splash Zone. The half-phases are shown in figure 6.5.

Table 6.3: Phases during a Horizontal Lift

Vertical Rigging	z	d
1 - In Air	0 m	0 m
2 - Through Splash Zone		
(a) - only flaps immersed	1.636 m	0.275 m
(b) - half immersed	3.000 m	1.639 m
(c) - fully immersed	4.378 m	3.081 m
3 - Fully Submerged	14.378 m	13.081 m

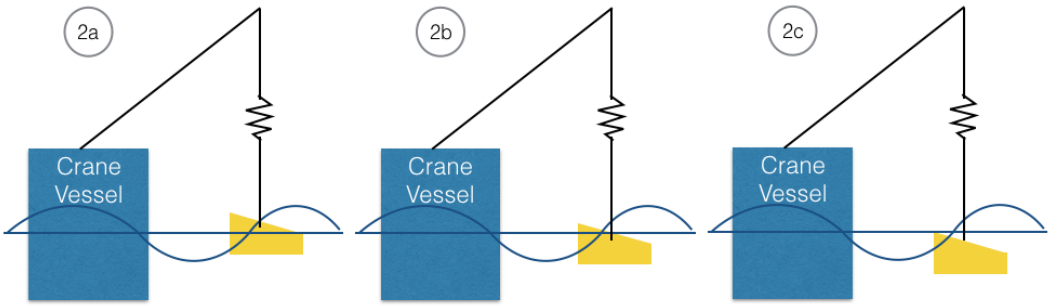

Figure 6.5: Lifting Through Splash Zone: (a) - only flaps immersed, (b) - half immersed, (c) - fully immersed

7 Operability

Weather conditions may affect and delay marine operations. The weather proved to be season dependent, and during summer it was more likely to observe lower significant wave heights and calmer weather windows compared to the winter season.

It can be interesting to know the average operability and the time for *waiting on weather (WOW)* for the specific operation field during the planning process. The determined weather criteria, based on the resulting force acting on the system during the lift, could give an estimate of when the operation can and cannot be carried out.

In order to be able to differentiate between season variation, the data sets were separated into four seasons; spring, summer, autumn and off-season/winter. Observed significant wave heights during each season were stored in separate vectors. To fulfil the *first* criterion in equation (3.4) where $Hs \leq Hs_{WF}$, the Hs in each season vector was compared with given Hs_{WF}. The total length of the calm and storm periods were stored in two segregated vectors. To fulfil the *second* criterion in equation (3.4) where $\tau_c \geq T_R$, the length of the periods in the two segregated vectors was compared to given T_R. If $(Hs \leq Hs_{WF}) \cap (\tau_c \geq T_R)$ the length of the period was stored in a *Calm* vector. If $(Hs \leq Hs_{WF}) \cap (\tau_c < T_R)$ the data was stored in a *Calm-Wait* vector. If $(Hs > Hs_{WF}) \cap (\tau_c \geq T_R)$ the data was stored in a *Storm-Wait* vector, and if $(Hs > Hs_{WF}) \cap (\tau_c < T_R)$ the data was stored in a *Storm* vector. The categories can be seen in figure 7.1 and 7.2 for Heidrun and Tanzania respectively, where segregation of seasons are not included.

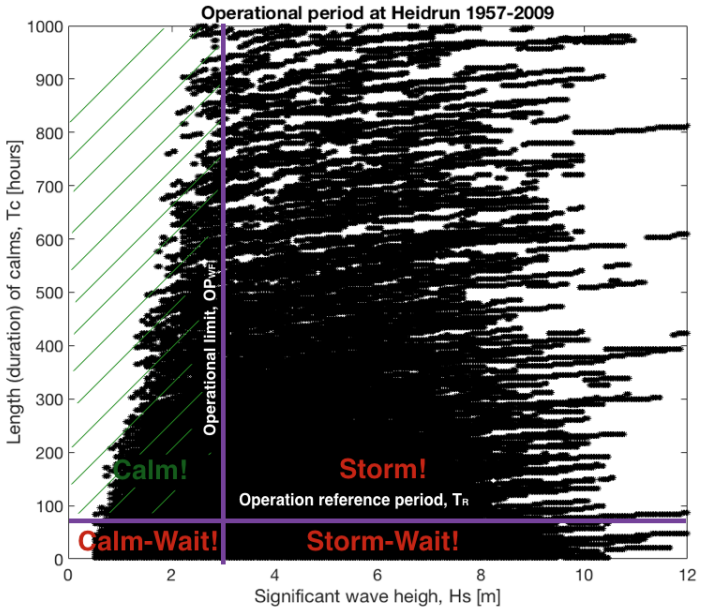

Figure 7.1: Observed length of calms against Hs at Heidrun, with categories

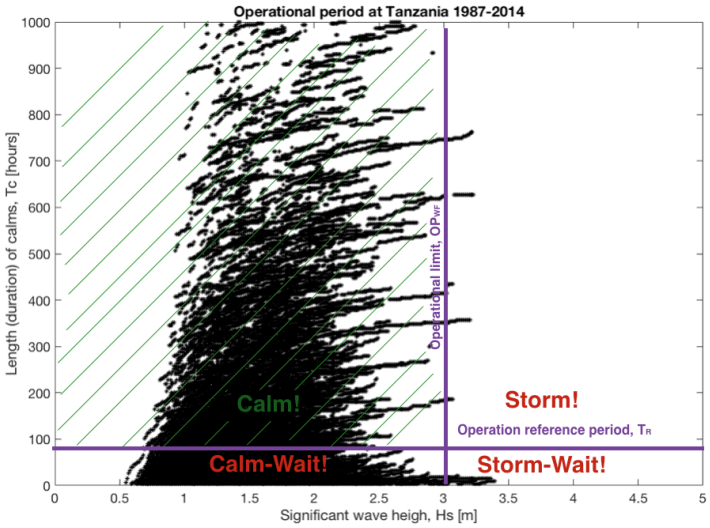

Figure 7.2: Observed length of calms against Hs at Tanzania, with categories

Season variation of the wave conditions were made visible by plotting observed length of calms against significant wave height for each season. This is shown in figure 7.3 and 7.3 for Heidrun and Tanzania respectively.

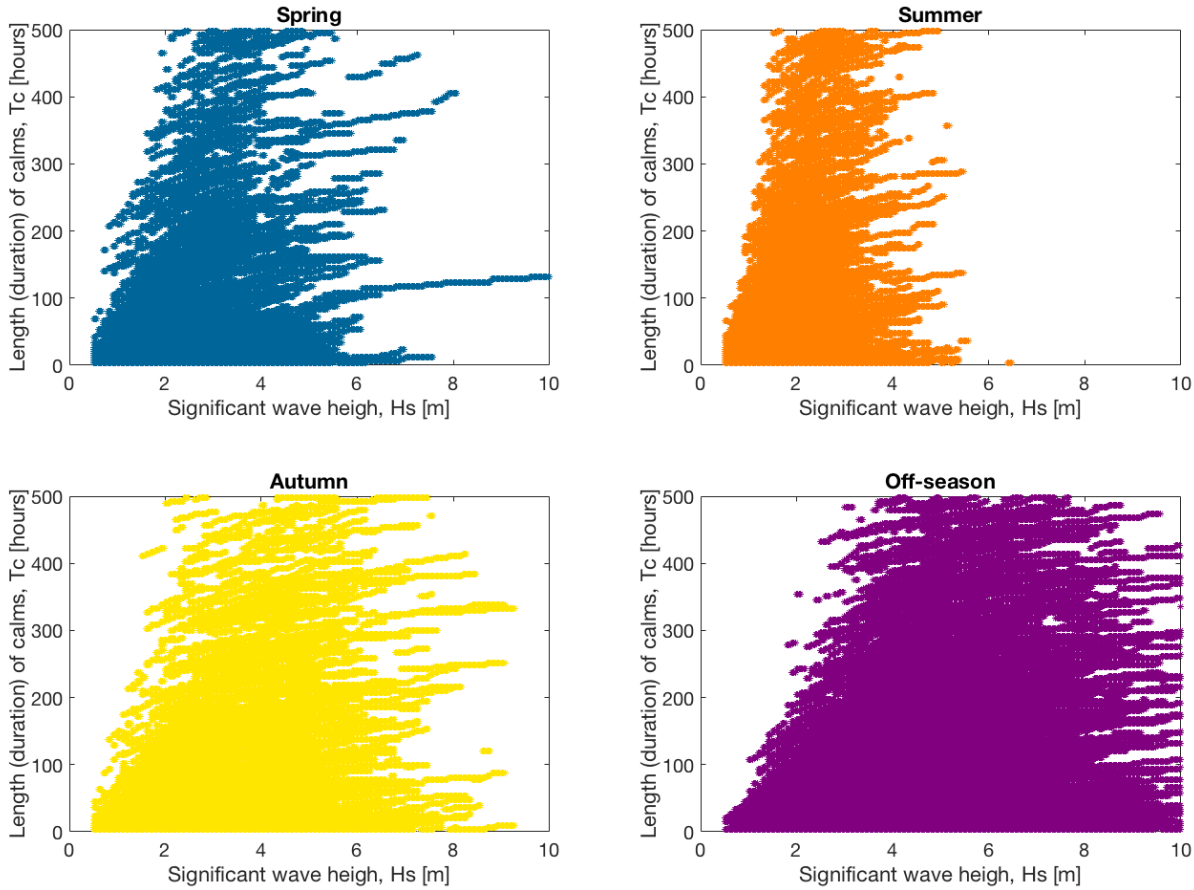

Figure 7.3: Observed length of calms against Hs for various seasons at Heidrun

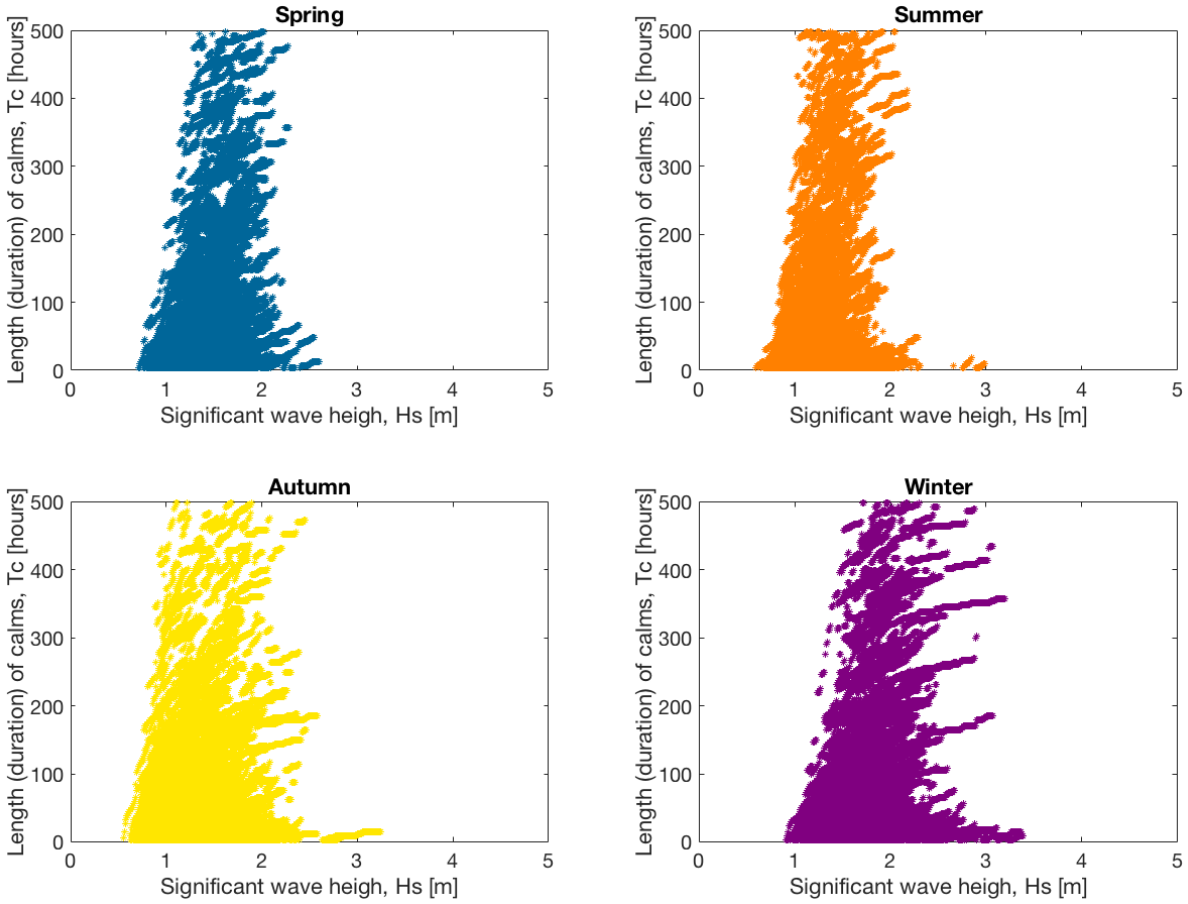

Figure 7.4: Observed length of calms against Hs for various seasons at Tanzania

Average operability for the marine operation was found by summing the calm periods with longer duration than the reference period, and divide it by the total amount of hours during each season. The average operational downtime will be the average of the operational downtime, which was found by summing the storm periods and the calm periods of lower duration than the reference period.

7.1 Heidrun

A level B marine operation with Hs_{LIM} of 2m and T_R less than 12 hours has an α-factor of 0.8. Thus, Hs_{WF} was calculated to be 1.8m. The probability that the operation could be performed during the different seasons with these operational criteria, can be found in table 7.1. Table 7.2 shows the operation downtime, which is how much one has to *wait on weather* for an identical operation.

Table 7.1: Average Operability at Heidrun, Hs_{LIM} = 2m

	Spring	Summer	Autumn	Off-season
Operability	**40.0 %**	**63.3 %**	**24.3 %**	**8.2 %**

Table 7.2: Average Downtime at Heidrun, Hs_{LIM} = 2m

Downtime	Spring	Summer	Autumn	Off-season
Calm-Wait	1.3 %	0.8 %	1.2 %	0.9 %
Storm-Wait	1.0 %	1.1 %	0.7 %	0.2 %
Storm	57.7 %	34.8 %	73.8 %	90.7 %
WOW	**60.0 %**	**36.7 %**	**75.7 %**	**91.8 %**

When the operational wave criterion was increased to 3m, the α-factor was 0.82. Thus Hs_{WF} was 2.46m and the operability and downtime for the operation are listed in table 7.3 and 7.4 respectively.

Table 7.3: Average Operability at Heidrun, Hs_{LIM} = 3m

	Spring	Summer	Autumn	Off-season
Operability	**71.2 %**	**88.1 %**	**52.5 %**	**28.4 %**

Table 7.4: Average Downtime at Heidrun, Hs_{LIM} = 3m

Downtime	Spring	Summer	Autumn	Off-season
Calm-Wait	0.7 %	0.2 %	1.0 %	1.3 %
Storm-Wait	1.2 %	0.8 %	1.0 %	0.6 %
Storm	26.9 %	10.9 %	45.5 %	69.7 %
WOW	**28.8 %**	**11.9 %**	**47.5 %**	**71.6 %**

The operability for a marine operation with T_R of 12 hours and various Hs-criteria, is shown in figure 7.5, for different seasons.

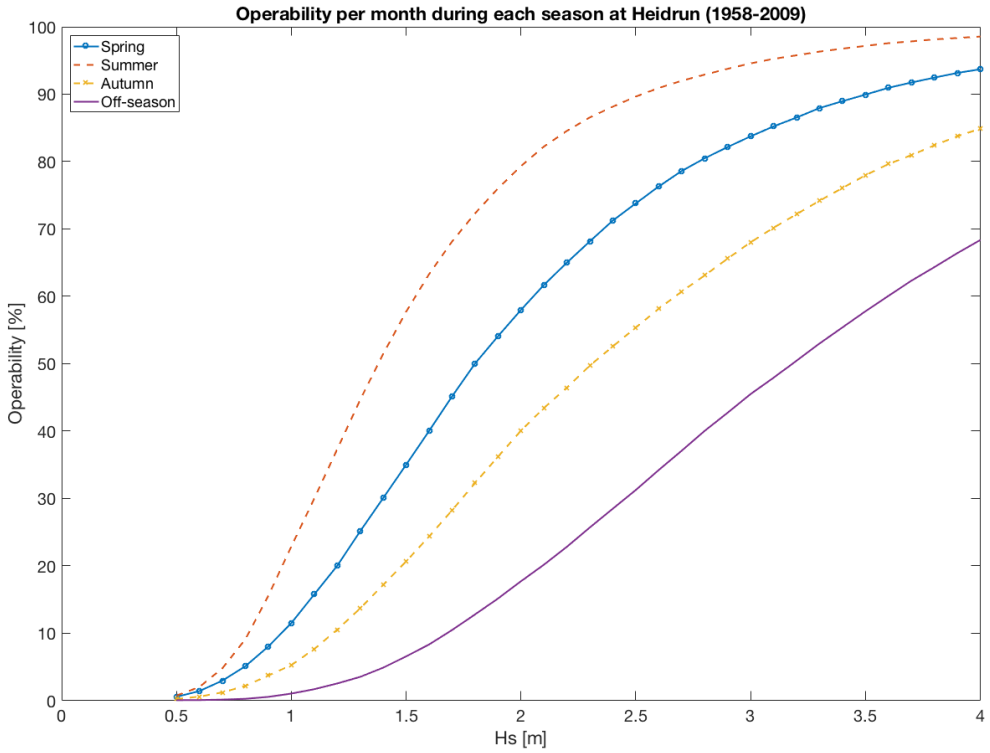

Figure 7.5: Operability per month during each season at Heidrun

7.1.1 Heidrun: Distribution of Calm Periods

A probability density function of length of calms at Heidrun fitted a Weibull distribution with scale γ- and shape β parameters as listed in table 7.5.

Table 7.5: Weibull distribution parameters fitting the calm periods at Heidrun

Hs_{LIM}	Parameters	Spring	Summer	Autumn	Off-season
2 m	Scale - γ	57.7	85.8	48.2	36.6
	Shape - β	1.26	1.16	1.25	1.50
3 m	Scale - γ	103.5	203.3	75.3	49.8
	Shape - β	1.06	0.96	1.10	1.28

The mean and standard deviation of the length of calms that fitted the Weibull distribution when Hs_{LIM} was 3m, are listed in table 7.6. The mean and standard deviation obtained from the real data set can be found in the same table.

Table 7.6: Mean and standard deviation of length of calms for distribution and data set at Heidrun [hours]

		Spring	Summer	Autumn	Off-season
Distribution	Mean	101.0	207.1	72.6	46.2
	Std	95.2	216.1	66.1	36.5
Data set	Mean	100.8	207.4	72.2	45.7
	Std	103.9	229.3	77.2	42.6

A Weibull distribution of calms at Heidrun, during spring, for Hs_{LIM} = 2m, is visualised to the left in figure 7.6. The probability plot for the Weibull distribution with scale- and shape parameters found in table 7.5 for spring, is shown to the right in the same figure.

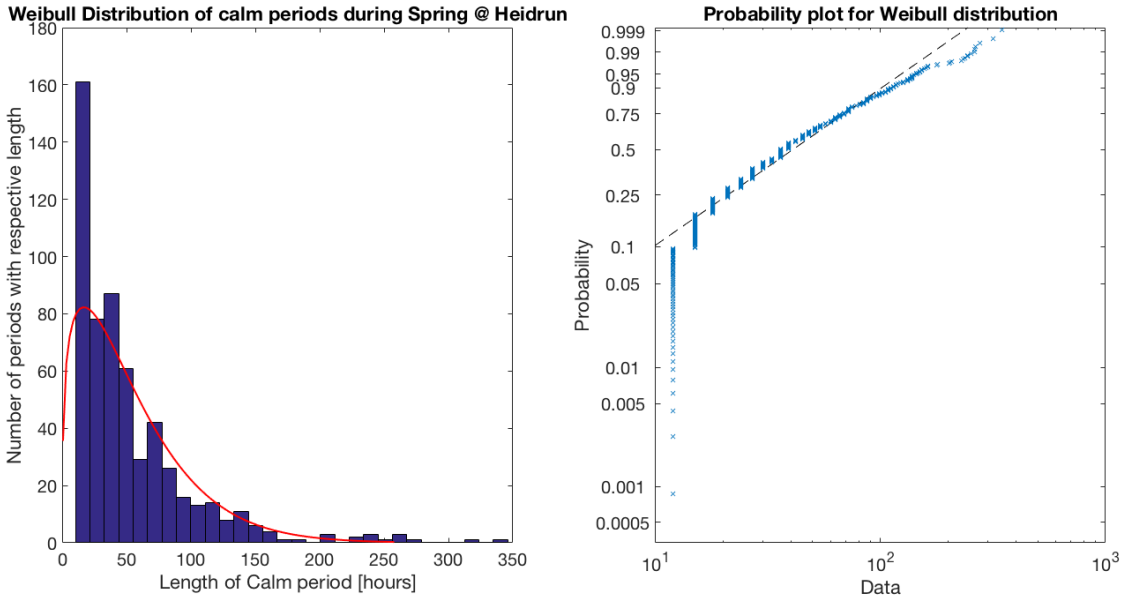

Figure 7.6: Weibull distribution of calm periods at Heidrun during spring

7.2 Tanzania Block 2

The level B marine operation had an operational wave height criterion Hs_{WF} of 1.8 m. The probability that the operation could be performed during the different seasons with these operational criteria, can be found in table 7.7. Table 7.8 shows the operation downtime.

Table 7.7: Average Operability at Tanzania, Hs_{LIM} = 2m

	Spring	Summer	Autumn	Winter
Operability	**81.2 %**	**91.4 %**	**84.6 %**	**47.7 %**

Table 7.8: Average Downtime at Tanzania, Hs_{LIM} = 2m

Downtime	Spring	Summer	Autumn	Winter
Calm-Wait	0.5 %	0.2 %	0.4 %	1.3 %
Storm-Wait	1.1 %	0.6 %	0.8 %	1.3 %
Storm	17.2 %	8.0 %	14.1 %	49.7 %
WOW	**18.8%**	**8.8 %**	**15.3 %**	**52.3 %**

When the operational wave criterion was increased to 3m, Hs_{WF} was found to be 2.46m. The operation operability and downtime are listed in table 7.9 and 7.10 respectively.

Table 7.9: Average Operability at Tanzania, Hs_{LIM} = 3m

	Spring	Summer	Autumn	Winter
Operability	**99.6 %**	**99.8 %**	**99.7 %**	**97.7 %**

Table 7.10: Average Downtime at Tanzania, Hs_{LIM} = 3m

Downtime	Spring	Summer	Autumn	Winter
Calm-Wait	0.01 %	0 %	0 %	0.08 %
Storm-Wait	0.05 %	0.02 %	0.06 %	0.37 %
Storm	0.30 %	0.18 %	0.25 %	1.89 %
WOW	**0.36 %**	**0.2 %**	**0.31 %**	**2.34 %**

The operability for a marine operation with T_R of 12 hours and various Hs-criteria, is shown in figure 7.7, for different seasons.

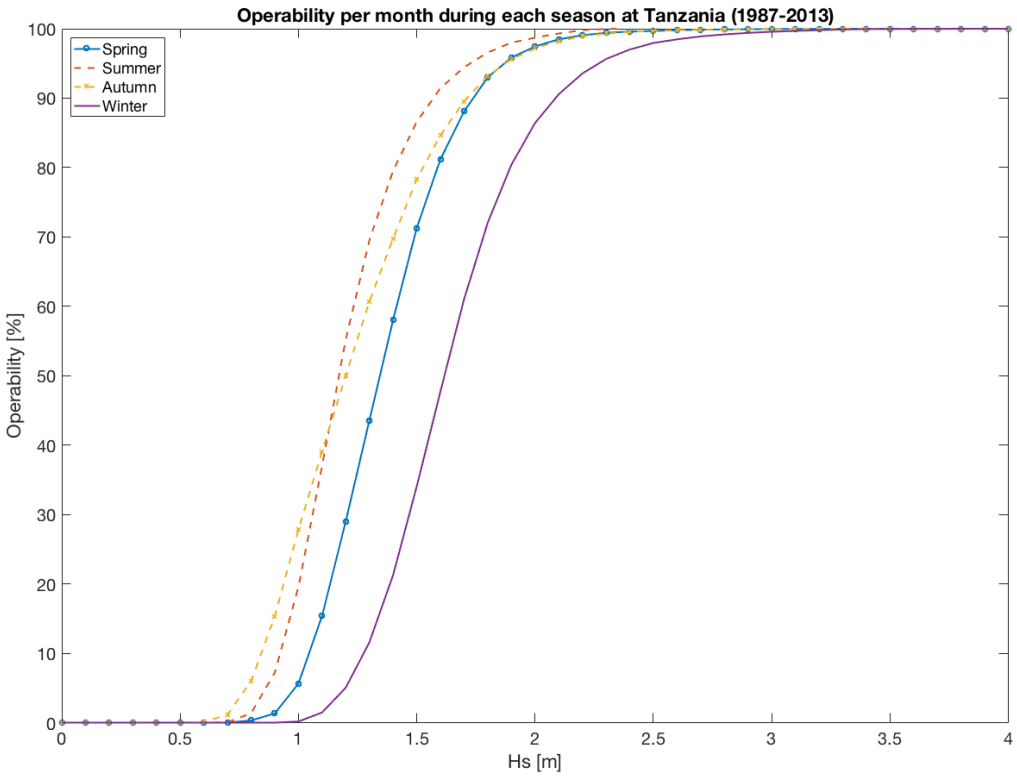

Figure 7.7: Operability per month during each season at Tanzania

7.2.1 Tanzania: Distribution of Calm Periods

A probability density function of length of calms at Tanzania fits a Weibull distribution with scale γ- and shape β parameters as listed in table 7.11.

Table 7.11: Weibull distribution parameters fitting the calm periods at Tanzania

Hs_{LIM}	Parameters	Spring	Summer	Autumn	Winter
2 m	Scale - γ	158.3	325.2	205.7	71.6
	Shape - β	0.82	0.76	0.73	1.06
3 m	Scale - γ	4 220	14 957	3 512	761
	Shape - β	0.88	1.06	0.61	0.81

The mean and standard deviation of the length of calms that fitted the Weibull distribution when HS_{LIM} was 3m, are listed in table 7.12. The mean and standard deviation obtained from the real data set can be found in the same table.

Table 7.12: Mean and standard deviation of length of calms for distribution and data set at Tanzania [hours]

		Spring	Summer	Autumn	Winter
Distribution	Mean	4 502	14 599	5 202	852
	Std	5 139	13 730	9 007	1 053
Data set	Mean	4 520	14 594	4 953	844
	Std	5 759	15 131	6 099	953

A Weibull distribution of calms at Tanzania, during spring, for Hs_{LIM} = 2m, is visualised to the left in figure 7.8. The probability plot for the Weibull distribution with scale- and shape parameters found in table 7.11 for spring, is shown to the right in the same figure.

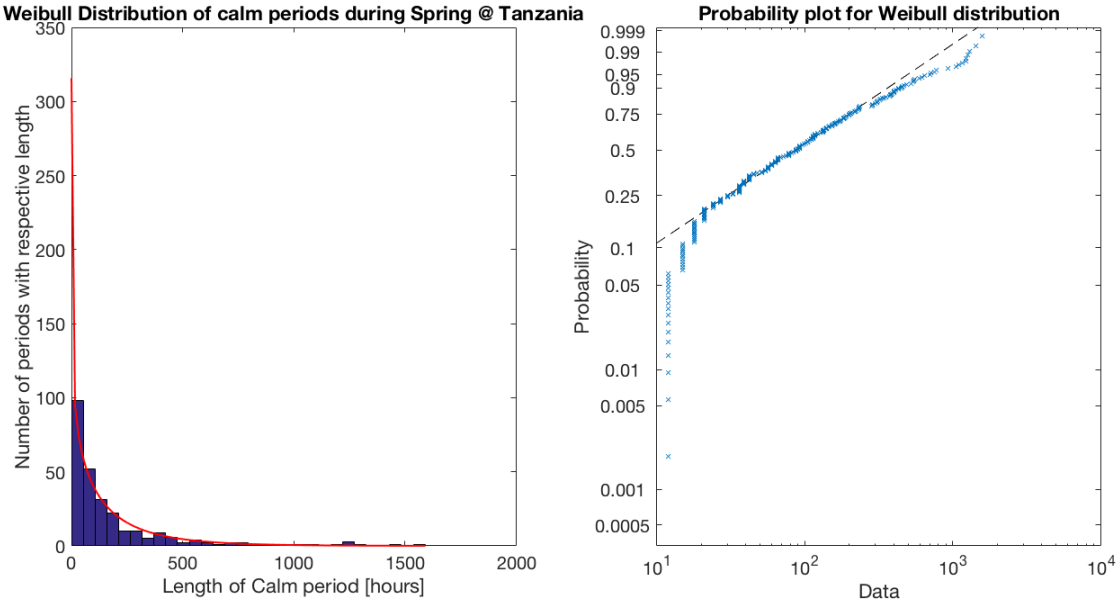

Figure 7.8: Weibull distribution of calm periods at Tanzania during spring

8 Hydrodynamic Approach

8.1 Linear Wave Theory

Due to the assumptions of incompressible and inviscid sea water, irrotational fluid motion, infinite water depth and that the pressure follows the Bernoulli equation, the velocity potential ϕ is given by equation (8.1).

$$\phi = \frac{g\zeta_a}{\omega} e^{kz} cos(\omega t - kx) \tag{8.1}$$

The wave kinematics decreases with depth z. The water particles will move in paths formed as circles. At sea surface the radius will equal the wave amplitude, and with large depth the radius will be close to zero. This is shown in figure 8.1.

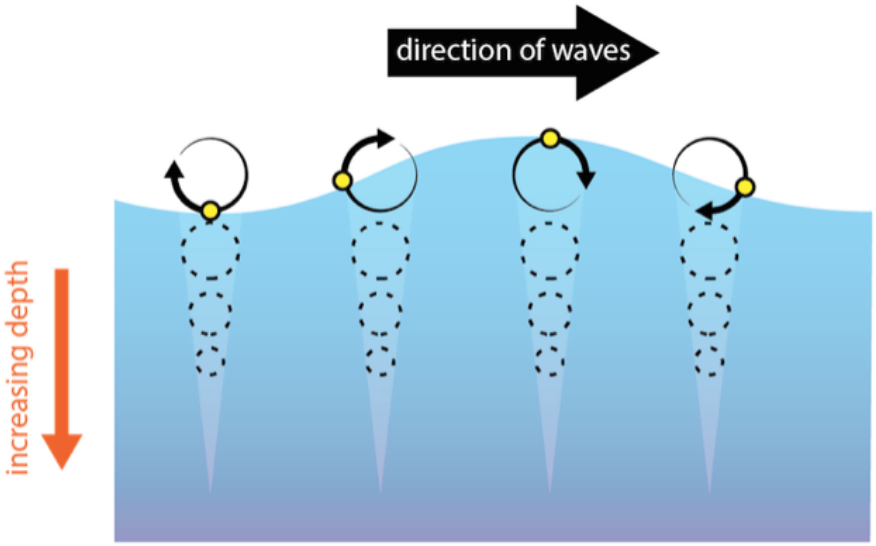

Figure 8.1: Water particles paths with water depth (TSI, 2016)

The velocity v_w and acceleration $\dot{v}_w$ is given by equation (8.2) and (8.3), where the wave number $k = \frac{\omega^2}{g}$, derived from the dispersion relation (Faltinsen, 1990).

$$v_w = \omega\zeta_a e^{kz} cos(\omega t - kx) \tag{8.2}$$

$$\dot{v}_w = -\omega^2\zeta_a e^{kz} sin(\omega t - kx) \tag{8.3}$$

The wave profile for a regular sinusoidal incident wave is given by equation (8.4). A regular wave propagates with permanent form. It has a distinct wave length, -period and -heigth (DNV GL, 2011b).

$$\zeta = \zeta_a sin(\omega t - kx) \tag{8.4}$$

8.2 Hydrodynamic Parameters

Hydrodynamic parameters can be determined by theoretical and/or experimental methods. Added mass and drag forces are important hydrodynamic forces caused by forced harmonic rigid body motions (Faltinsen, 1990). They depend on the body geometry, perforation, sharp edges, vicinity of free surface or sea bottom, oscillation, wave height and wave period (DNV GL, 2011b).

8.2.1 Added Mass Value

Added mass is associated with a mass of fluid that is accelerated by the object due to generation of surface waves (Rahman and Bhatta, 1993). Added mass may be highly dependent on the oscillation amplitude of the object.

Theoretical added mass values exist for simple geometries and can be found in table *A-2* in *DNV GL's Recommended Practice DNV-RP-H103, 2011b*, and is shown in figure 8.2. For realistic geometries experimental data has to be relied on (Nilsen, 2016). Added mass calculations based upon superposition, which is summation of contributions from each element, is not recommended if the structure is densely compounded. Due to oscillation amplitude dependency and interaction effects, an underestimation of the calculated values may be expected. Reduction in added mass due to perforation has to be considered. Added mass will be halved at 30% perforation (DNV GL, 2011b).

Table A-2 Analytical added mass coefficient for three-dimensional bodies in infinite fluid (far from boundaries). Added mass is $A_{ij}=\rho C_A V_R$ [kg] where V_R [m^3] is reference volume

Body shape		*Direction of motion*	C_A				V_R
Flat plates	Circular disc 	Vertical	$2/\pi$				$\frac{4}{3}\pi a^3$
	Elliptical disc 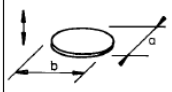	Vertical	*b/a*	C_A	*b/a*	C_A	$\frac{\pi}{6}a^2 b$
			∞	1.000	5.0	0.952	
			14.3	0.991	4.0	0.933	
			12.8	0.989	3.0	0.900	
			10.0	0.984	2.0	0.826	
			7.0	0.972	1.5	0.758	
			6.0	0.964	1.0	0.637	
	Rectangular plates 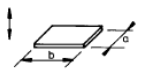	Vertical	*b/a*	C_A	*b/a*	C_A	$\frac{\pi}{4}a^2 b$
			1.00	0.579	3.17	0.840	
			1.25	0.642	4.00	0.872	
			1.50	0.690	5.00	0.897	
			1.59	0.704	6.25	0.917	
			2.00	0.757	8.00	0.934	
			2.50	0.801	10.00	0.947	
			3.00	0.830	∞	1.000	

Figure 8.2: Table of added mass coefficients for a three-dimensional body (DNV GL, 2011b)

The added mass value is given in *kilos* and can be found by equation (8.5). C_A and V_R can be found in the table above, where C_A is the dimensionless added mass coefficient and V_R is the reference

volume in kg. A_{ij} is the added mass force in i-direction due to acceleration in j-direction.

$$A_{ij} = \rho C_A V_R \tag{8.5}$$

Added mass will increase through splash zone when the object's projected area increases. Thereafter it will stay constant until it again will start to increase when the structure approaches the sea bottom (Nilsen, 2016).

8.2.2 Drag coefficient

Drag forces are flow resistance on submerged part of the structure and are related to relative velocity between object and water particles (Bøe, 2016). The drag force is based on a drag coefficient C_D which in reality has to be empirically determined. C_D is dependent on many parameters as Reynold number and Keulegan-Carpenter number. It is assumed that C_D is constant with depth for constand submerged projected area. This might not be realistic because drag is influenced by the presence of a current (Faltinsen, 1990). The drag coefficient can be found in table *B-2* in *DNV GL's Recommended Practice DNV-RP-H103, 2011b*, and is shown in figure 8.3. In oscillatory flow the drag coefficient C_D is generally $\geq$ 2.5 (DNV GL, 2011b).

Table B-2
Drag coefficient on three-dimensional objects for steady flow C_{DS}.
Drag force is defined as $F_D = \frac{1}{2}\rho C_{DS} S u^2$.

S = projected area normal to flow direction [m^2].
R_e = uD/ν = Reynolds number where D = characteristic dimension.

Geometry	*Dimensions*	C_{DS}
Rectangular plate normal to flow direction	B/H	
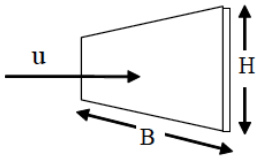	1 5 10 ∞	1.16 1.20 1.50 1.90
		$R_e > 10^3$

Figure 8.3: Table of drag coefficients on three-dimensional objects (DNV GL, 2011b)

8.3 Dynamic Equilibrium Equation

Dynamic loads vary with time and hence differ from static loads by implying a time dependent solution and introducing inertia loads throughout the structure (Langen and Sibjörnsson, 2009). The dynamic equilibrium equation is given by equation (8.6).

$$(m + m_a)\ddot{\eta}_3 + c\dot{\eta}_3 + k\eta_3 = F_3 sin(\omega t) \tag{8.6}$$

m = total mass of lifted object and rigging [kg]
m_a = added mass coefficient [kg]

c = damping coefficient [$\frac{kg}{s}$]
k = restoring coefficient [$\frac{kg}{s^2}$]
η_3 = translation in heave [m]
$\dot{\eta}_3$ = velocity in heave [$\frac{m}{s}$]
$\ddot{\eta}_3$ = acceleration in heave [$\frac{m}{a^2}$]
F_3 = excitation forces [N]

The lifted object will have a heave motion defined as $\eta = \eta_0 sin(\omega t - \varepsilon)$. η_0 is the vertical single amplitude motion of the lifted object and can be found by equation (8.7) and ε is the phase angle between wave and crane tip motion.

$$\eta_0 = \frac{F_3}{k} \cdot DAF \tag{8.7}$$

The dynamic amplification factor (DAF) accounts for global dynamic effects that might arise during a lifting operation (DNV GL, 2014). The DAF is a dimensionless number and is defined as the ratio between dynamic and static displacement (Langen and Sibjörnsson, 2009), and is calculated by equation (8.8), where ω_0 is the natural frequency.

$$DAF = \frac{1}{\sqrt{(1 - (\frac{\omega}{\omega_0})^2)^2 + \omega^2 \frac{c^2}{k^2}}} \tag{8.8}$$

Capacity checks have to be performed for the lift, an the following relation should be applied $DAF = \frac{F_{dyn}+F_{stat}}{F_{stat}} = \frac{F_{tot}}{Mg}$ (Bøe, 2016). Global dynamic load effects can be found by using the DAF.

The natural frequency ω_0 is dependent on the system's mass, added mass and stiffness, and is found by equation (8.9).

$$\omega_0 = \sqrt{\frac{k}{(m + m_a)}} \tag{8.9}$$

The damping ratio is denoted as ξ and is the ratio between actual and critical damping, and can be calculated by equation (8.10). The critical damping coefficient $c_{cr} = 2\sqrt{km} = 2m\omega$ and is used to categorise the damping to *critical* ($c = c_{cr}$), *supercritical* ($c > c_{cr}$) or *subcritical* ($c < c_{cr}$) (Langen and Sibjörnsson, 2009).

$$\xi = \frac{c}{c_{cr}} = \frac{c}{2(m + m_a)\omega_0} \tag{8.10}$$

8.4 Static and Dynamic Equilibrium

Static load in the hoisting line $F_{line,static}$ will be the sum of the weight of the lifted object and rigging equipment, the line's mass and the buoyancy force, as shown in the static equilibrium equation (8.11). A porous object will be filled with water when it is submerged, thus the mass will increase slowly with time.

$$F_{line,static} = Mg + m(t)g - F_{B,mean} \tag{8.11}$$

The *total line force* is the sum of static and dynamic line force as shown in equation (8.12).

$$F_{line,tot} = F_{line,static} + F_{line,dynamic} = Mg + m(t)g - F_{B,mean} + K(\eta_{ct} - \eta) \tag{8.12}$$

Dynamic equilibrium can be found by adding the inertia-, drag-, slamming-, varying buoyancy- and static forces, as shown in equation (8.13) (Larsen, 2016).

$$\begin{aligned} M\ddot{\eta} &= F_I + F_d + F_S + F_B + F_{line,dyn} \\ &= -\rho C_A V \ddot{\eta} + \rho V(1 + C_A)\dot{v} + \frac{1}{2}\rho C_D S(v - \dot{\eta})|v - \dot{\eta}| \\ &\quad + \frac{1}{2}\rho C_S A_p(\dot{\zeta} - \dot{\eta})^2 + \rho g A_w \zeta + K(\eta_{ct} - \eta) \end{aligned} \tag{8.13}$$

By rearranging equation (8.13) we get dynamic equilibrium as defined in equation (8.14), where added mass A equals $\rho C_A V_R$.

$$\begin{aligned} (M + A)\ddot{\eta} + K\eta &= \rho V_R(1 + C_A)\dot{v} + \frac{1}{2}\rho C_D S(v - \dot{\eta})|v - \dot{\eta}| \\ &\quad + \frac{1}{2}\rho C_S A_p(\dot{\zeta} - \dot{\eta})^2 + \rho g A_W \zeta + K\eta_{ct} \end{aligned} \tag{8.14}$$

M = mass of lifted object	A_w = waterplane area of object
ρ = sea water density	ζ = wave elevation
C_A = added mass coefficient	$\dot{\zeta}$ = wave velocity
V_R = added mass reference volume	η_{ct} = crane tip vertical motion
K = stiffness of hoisting cable	η = dynamic vertical motion
C_D = drag coefficient in oscillatory flow	$\dot{\eta}$ = dynamic vertical velocity
S = projected area normal to force direction	$\ddot{\eta}$ = dynamic vertical acceleration
C_S = slamming coefficient	v = fluid particle vertical velocity
A_p = horizontal projected area of object	$\dot{v}$ = fluid particle vertical acceleration

8.5 Simplified Method

The Simplified Method for estimation of hydrodynamic forces and tension in the hoisting line can be applied for objects lowered through the water surface and down to the sea bottom. The aim with this method is to find allowable sea states limited by capacity of crane and lifting equipment and to achieve simple conservative estimates of the forces acting on the object as; drag-, inertia-, water entry (slamming)- and varying buoyancy forces. By using the Simplified Method one assumes that the wave length is large relative to the horizontal length of the lifted object, that the vertical motion of the object follows the crane tip motion ($\eta_{ct} = \eta$), and that the vertical motion of the object dominates and all other motions can be disregarded (DNV GL, 2011b). Thus added mass force in heave A_{33} and drag force in vertical direction are of interest. By utilising the Simplified Method, tension in

hoisting lines and the limiting criteria of crane operations can be found in an efficient way (Larsen, 2016).

According to DNV GL, the Simplified Method can be applied for the criteria shown in figure 8.4, and is recommended when the length of the body is 4 · L, where L is the wave length (Bøe, 2016).

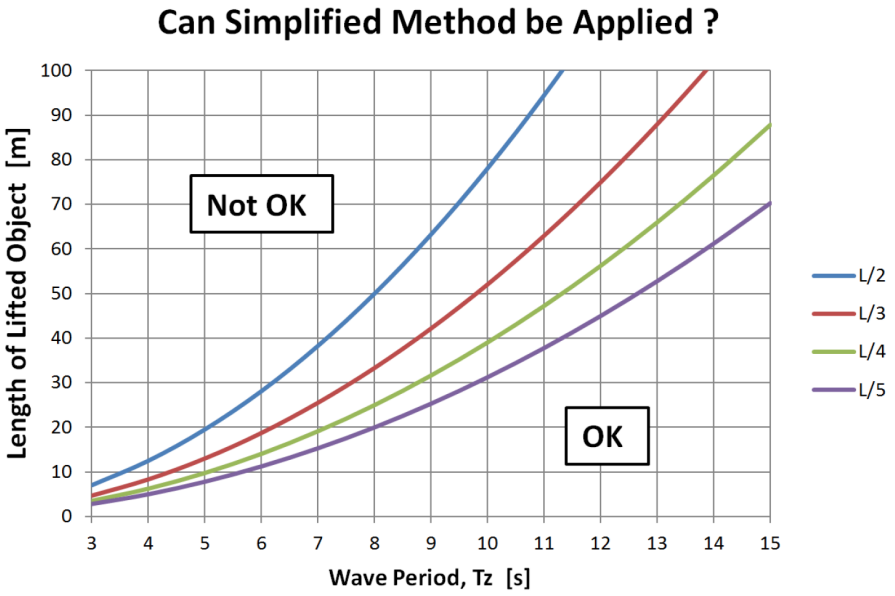

Figure 8.4: Can Simplified Method be Applied?

8.5.1 Wave Kinematics

The wave particle velocity and acceleration can be found by equation (8.15) and (8.16) respectively. The equations are derived from linear wave theory where $\omega = \frac{2\pi}{T_z}$, $k = \frac{\omega^2}{g}$ and d is the distance from sea surface to the centre of gravity of submerged part of object (Larsen, 2016).

$$v_w = \zeta_a \cdot (\frac{2\pi}{T_z}) \cdot e^{-\frac{4\pi^2 d}{T_z^2 g}} \tag{8.15}$$

$$\dot{v}_w = \zeta_a \cdot \left(\frac{2\pi}{T_z}\right)^2 \cdot e^{-\frac{4\pi^2 d}{T_z^2 g}} \tag{8.16}$$

For an operation where the duration of crossing the splash zone is less than 30 minutes, the wave amplitude $\zeta_a = 0.9 \cdot H_S$, and the zero-crossing period T_z is defined by equation (8.17) (DNV GL, 2011b).

$$T_z = 2\pi\sqrt{\frac{M_0}{M_Z}} \tag{8.17}$$

8.5.2 Drag Force

Drag forces are caused by relative velocity between lifted object and water particles. The drag force can be calculated by equation (8.18) (Larsen, 2016), where the drag coefficient C_D can be found in table *B-2* in *DNV GL's Recommended Practice DNV-RP-H103, 2011b*, and is shown in figure 8.3.

$$F_D = \frac{1}{2} \cdot \rho \cdot C_D \cdot A_p \cdot v_r^2 \tag{8.18}$$

ρ = density of sea water
C_D = drag coefficient in oscillatory flow of submerged part of object
A_p = projected area of submerged part of object in a horizontal plane
v_r = characteristic vertical relative velocity between object and water particles, and is found by equation (8.19).

$$v_r = v_c + \sqrt{\dot{\eta}_{ct}^2 + v_w^2} \tag{8.19}$$

v_c = hook hoisting/lowering velocity
$\dot{\eta}_{ct}$ = characteristic single amplitude vertical velocity of the crane tip
v_w = characteristic vertical water particle velocity

8.5.3 Water Entry (Slamming) Force

Slamming forces are impulse loads with high pressure peaks that occur during impact between an object and the water surface. Slamming will occur when an object is lifted trough the splash zone and hits the water with a high velocity (Faltinsen, 1990). The slamming force can be calculated by equation (8.20), where A_S and C_S are the relevant slamming area and -coefficient respectively (Larsen, 2016).

$$F_S = \frac{1}{2} \cdot \rho \cdot C_s \cdot A_s \cdot v_s^2 \tag{8.20}$$

C_S = slamming coefficient which may be determined by theoretical and/or experimental methods. C_S should not be taken less than 5.0 (DNV GL, 2011b)
A_S = slamming area, identical projected area of submerged part of object in a horizontal plane
v_S = slamming impact velocity, which is identical to the relative velocity between object and water particles v_r, calculated in section 8.5.2.

The slamming coefficient C_S can be found theoretically by equation (8.21), where $\frac{dA_{33}^{\infty}}{dh}$ is the rate of change of added mass with submergence.

$$C_S = \frac{2}{\rho A_p} \frac{dA_{33}^{\infty}}{dh} \tag{8.21}$$

8.5.4 Inertia Force

Inertia forces are caused by crane tip acceleration and acceleration of water particles. The total inertia force is here a combination of inertia-, Froude-Kriloff- and diffraction forces, and calculated by equation (8.22) (Bøe, 2016). The relation between the crane tip- and water particle accelerations is visualised in figure 8.5.

$$F_I = \sqrt{[(M + A_{33})\ddot{\eta}_{ct}]^2 + [(\rho V + A)\dot{v}_w]^2} \tag{8.22}$$

M = mass of object
A_{33} = added mass in heave
$\ddot{\eta}_{ct}$ = crane tip acceleration
V = volume of displaced water
$\dot{v}_w$ = water particle acceleration

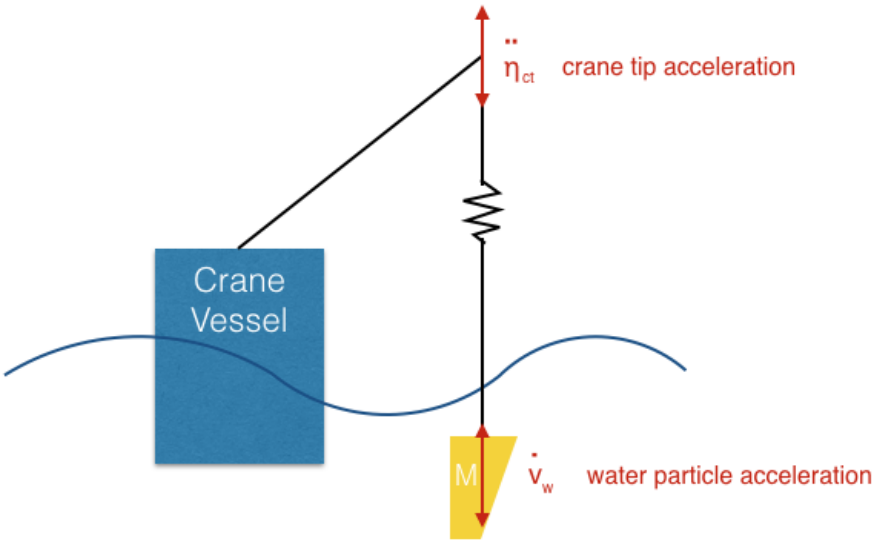

Figure 8.5: Relation between crane tip- and water particle acceleration

8.5.5 Varying Buoyancy Force

When an object is lowered into the ocean, a buoyancy force will instantly affect the lifting load. The buoyancy force varies due to change in geometry and buoyancy relative to water surface elevation. The varying buoyancy force F_B is calculated by equation (8.23), where wave amplitude ζ_a and crane tip motion η_{ct} are important parameters, and assumed statistically independent (Larsen, 2016). The relation between the crane tip motion and the wave amplitude is visualised in figure 8.6.

$$F_B = \rho \cdot \delta V \cdot g \tag{8.23}$$

δV is the varying volume due to oscillation and is given by equation (8.24), where A_w is the mean

water line area in the wave surface zone.

$$\delta V = A_w \cdot \sqrt{\zeta_a^2 + \eta_{ct}^2} \tag{8.24}$$

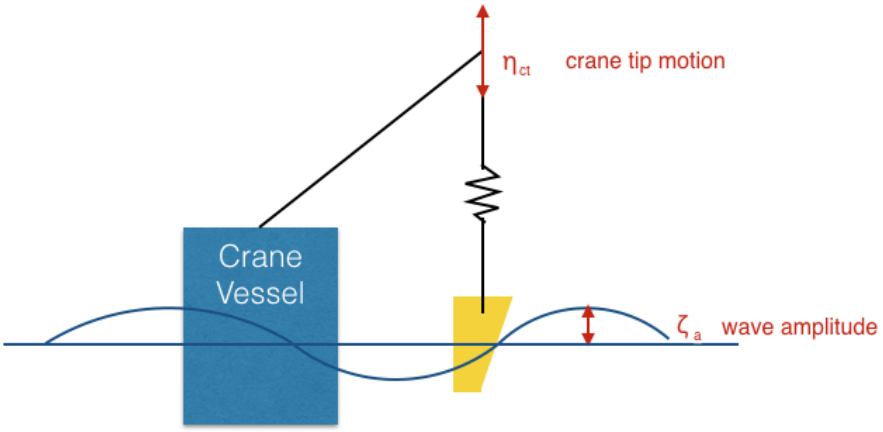

Figure 8.6: Relation between crane tip motion and wave amplitude

8.5.6 Resulting Force

Using the Simplified Method, the resulting hydrodynamic force is a combination of the drag- and inertia forces, and slamming- and varying buoyancy forces, as indicated in equation (8.25) (Larsen, 2016).

$$F_{Hyd} = \sqrt{(F_D + F_S)^2 + (F_I - F_B)^2} \tag{8.25}$$

The drag and slamming forces are summarised because they can occur simultaneously. Varying buoyancy and buoyancy forces will compensate for inertia and mass forces, hence they are subtracted.

The resulting force is the sum of the mass force, the buoyancy force and the total hydrodynamic forces. The mass force is the weight of the lifted object with rigging equipment. The resulting force is calculated by equation (8.26).

$$F_{Res} = Mg - F_{buoy} + F_{Hyd} \tag{8.26}$$

9 Establishment of Hydrodynamic Parameters

To be able to calculate the total forces acting on the cover during the different phases of the lift, hydrodynamic parameters as added mass and drag force were calculated. Added mass was calculated by following DNV GL's procedure for a rectangular plate, as further explained in *section 8.2.1 Added mass*. C_A was found by interpolating in table A-2 for rectangular plates, shown in figure 8.2. For rectangular plates $V_R = \frac{\pi}{4}a^2b$, and the added mass value was calculated by equation (9.1).

$$A_{33} = \rho \cdot C_A \cdot \frac{\pi}{4} \cdot a^2 b \tag{9.1}$$

There is no linear relation between the added mass and the projected area $A_p = ab$. Thus, the total added mass value would differentiate depending on how the projected area was divided. Two methods of dividing the projected area were further looked into; the *Superposition-Technique* and the *Plate-Technique*.

Due to the cover geometry, water was trapped inside the cover and affected the added mass. Correction of a three-dimensional body with vertical sides was not applied. Effect of perforation on the added mass was neither taken into account because of a perforation rate p less than 5% (DNV GL, 2011b).

The drag force is proportional to the projected area S, thus the force would not differ with divided area, superposition was allowed at any time.

$$F_D = \frac{1}{2} \cdot \rho \cdot C_{DS} \cdot S \cdot v_r^2 \tag{9.2}$$

The characteristic vertical relative velocity between object and water particles v_r was found by equation (8.19). It was assumed that the lifting speed v_c is 0.3 m/s, and that the crane tip velocity v_{ct}, in worst-case scenario, was identical to the characteristic vertical water particle velocity v_w. v_w is dependent on the distance from the sea surface to the lifted object's centre of gravity and calculated by equation (8.15).

The wave amplitude ζ_a is 0.9 · Hs, and with an Hs of 3 m, ζ_a was calculated to be 2.7m. T_z was determined to be 8 seconds.

9.1 Vertical Rigging

The projected areas used to calculate the added mass value and the drag force are shown in figure 9.1 and 9.2 respectively. The cover roof height increases with a slope of 0.211 per meter. Thus, a and H_{ver} in figure 9.1 and 9.2 will vary with submerged depth as for the linear equation (9.3), where $0 \leq z \leq 13$ m.

$$a = \frac{(4.378 - 1.636)}{13} z = 0.211z \tag{9.3}$$

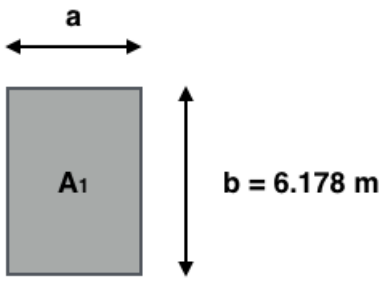

Figure 9.1: Projected area for added mass - vertical lift

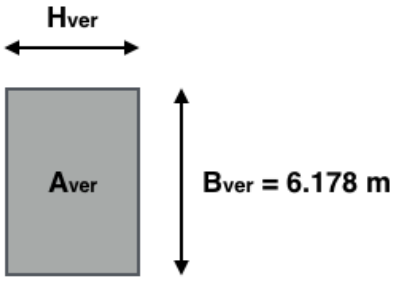

Figure 9.2: Projected area for drag force - vertical lift

9.1.1 Through Splash Zone

The lift will go through two *half-phases* crossing the splash zone; half immersed and fully immersed.

9.1.1.1 (a) Half Immersed

The cover was half immersed when submerged depth z was 6.5 m, as shown in figure 9.3. The parameters used to calculate the added mass value and the drag force are listed in table 9.1.

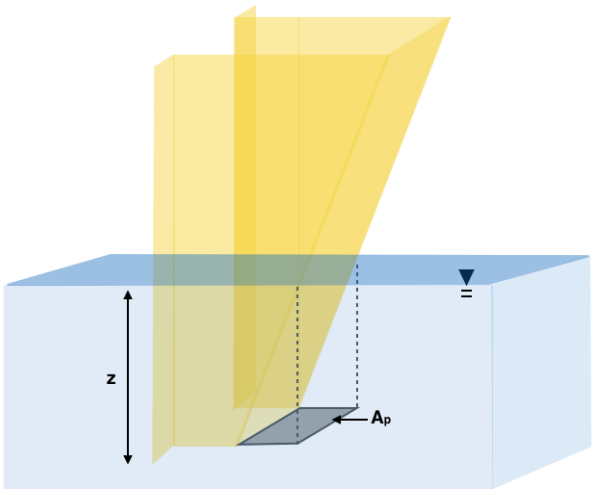

Figure 9.3: Vertical Lift Through Splash Zone, (a) half immersed

Table 9.1: Hydrodynamic parameters for vertical lift through splash zone (a) - half immersed

Added mass		Drag force	
Parameters	**Values**	**Parameters**	**Values**
a	1.371 m	H_{ver}	1.371 m
b	6.178 m	B_{ver}	6.178 m
$\frac{b}{a}$	4.507	$\frac{B_{ver}}{H_{ver}}$	4.507
C_A	0.885	S	8.470 m^2
V_R	9.150 kg	C_{DS}	1.195
		v_w	2.041 m/s
		v_r	3.186 m/s
A_{33}	**8 300 kg**	**F_D**	**52 664 N**

9.1.1.2 (b) Fully Immersed

The cover was fully immersed through splash zone when depth z was 13 m, as shown in figure 9.4. The parameters used to calculate the added mass value and the drag force are listed in table 9.2.

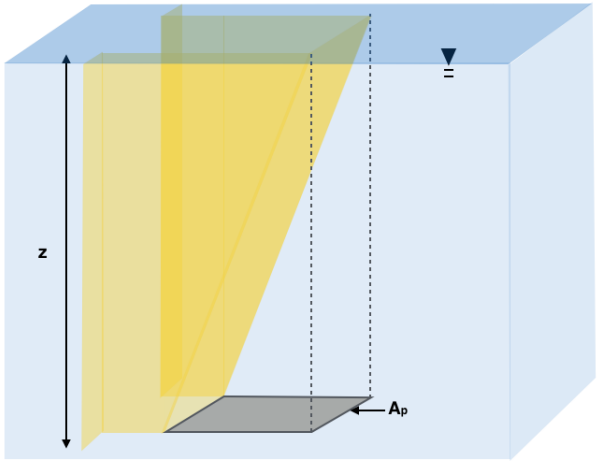

Figure 9.4: Vertical Lift Through Splash Zone, (b) fully immersed

Table 9.2: Hydrodynamic parameters for vertical lift through splash zone (b) - fully immersed

Added mass		**Drag force**	
Parameters	**Values**	**Parameters**	**Values**
a	2.742 m	H_{ver}	2.742
b	6.178 m	B_{ver}	6.178 m
$\frac{b}{a}$	2.253	$\frac{B_{ver}}{H_{ver}}$	2.253
C_A	0.779	S	16.94 m^2
V_R	36.481 kg	C_{DS}	1.173
		v_w	1.340 m/s
		v_r	2.195 m/s
A_{33}	**29 130 kg**	**F_D**	**49 051 N**

9.1.2 Fully Submerged

The cover was fully submerged with submerged depth z of 23 m, as shown in figure 9.5. The calculated hydrodynamic parameters are listed in table 9.3.

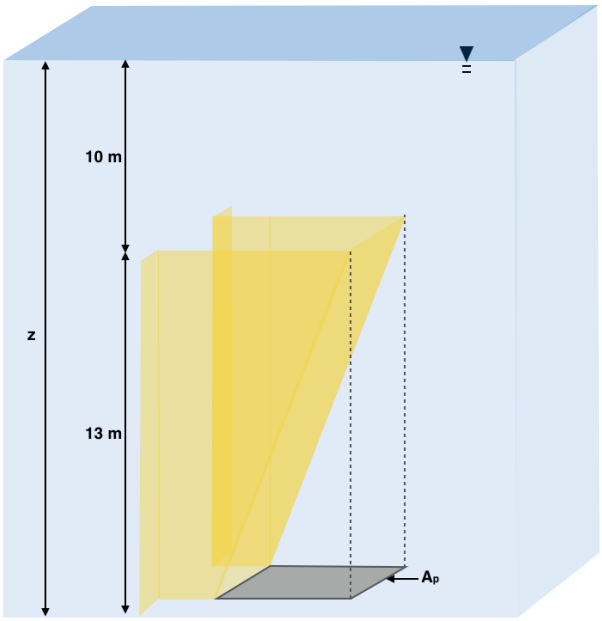

Figure 9.5: Vertical Lift - Fully Sumberged

Table 9.3: Hydrodynamic parameters for vertical lift - fully submerged

Added mass		Drag force	
Parameters	**Values**	**Parameters**	**Values**
a	2.742 m	H_{ver}	2.742
b	6.178 m	B_{ver}	6.178 m
$\frac{b}{a}$	2.253	$\frac{B_{ver}}{H_{ver}}$	2.253
C_A	0.779	S	16.94 m^2
V_R	36.481 kg	C_{DS}	1.173
		v_w	0.714 m/s
		v_r	1.310 m/s
A_{33}	**29 130 kg**	**F_D**	**17 484 N**

9.2 Horizontal Rigging

For a horizontal rigging the cover will be lowered through the splash zone horizontally with the "flaps" first. Water will be trapped inside the cover and affect the added mass. The total added mass is the sum of the added mass of the cover and the mass of the trapped water.

9.2.1 Through Splash Zone

The lift will go through three *half-phases* crossing the splash zone; only flaps immersed, half immersed, fully immersed.

9.2.1.1 (a) Only flaps immersed

During this half phase the cover "flaps" were the only parts that were immersed, and the submerged depth z varied between 0 m and 1.636 m, as shown in figure 9.6.

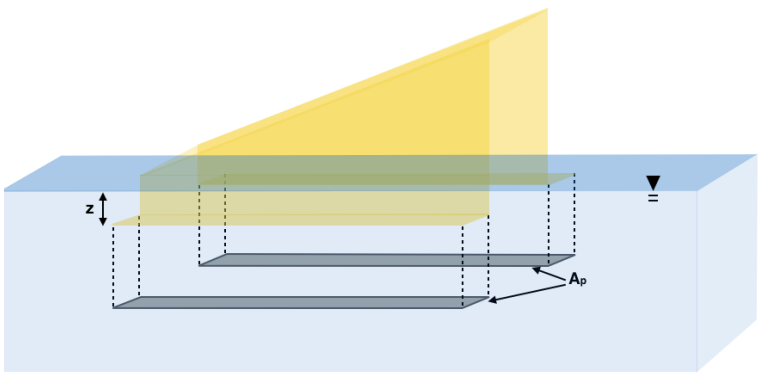

Figure 9.6: Horizontal Lift Through Splash Zone, (a) only flaps immersed

The projected area used to determine the added mass value and the drag force will have dimensions as shown in figure 9.7 and 9.8 respectively. The calculated hydrodynamic parameters are listed in table 9.4. $A_{33,tot}$ and $F_{D,tot}$ are the total added mass value and the total drag force for two submerged flaps.

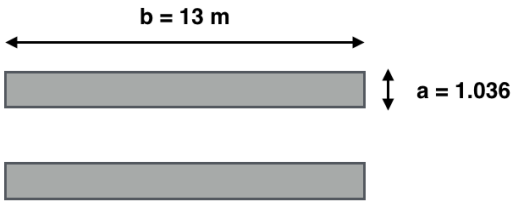

Figure 9.7: Projected area for added mass - Horizontal Lift Through Splash Zone (a)

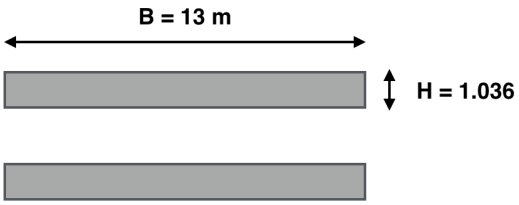

Figure 9.8: Projected area for drag force - Horizontal Lift Through Splash Zone (a)

Table 9.4: Hydrodynamic parameters for horizontal lift through splash zone (a) - only flaps immersed

Added mass		**Drag force**	
Parameters	**Values**	**Parameters**	**Values**
a	1.036 m	H	1.036 m
b	13 m	B	13 m
$\frac{b}{a}$	12.548	$\frac{B}{H}$	12.548
C_A	0.964	S	13.468 m^2
V_R	10.959 kg	C_{DS}	2.053
A_{33}	10 828 kg	v_w	2.084 m/s
		v_r	3.248 m/s
		F_D	149 492 N
$A_{33,tot}$	**21 656 kg**	**$F_{D,tot}$**	**298 984 N**

9.2.1.2 (b) Half Immersed

For further immersing of the cover, the cover roof height increased and affected the projected area. When $1.636 \leq z \leq 4.378$ m, x in figure 9.9 and 9.10 was found by equation (9.4).

$$x = \frac{13}{4.378 - 1.636} \cdot (z - 1.636) = 4.741 \cdot (z - 1.636) \tag{9.4}$$

In this specified lifting scenario there were two ways to determine the added mass force. One was to use superposition, where the projected area of the "flaps" and the "mid-area" were used separately to calculate the added mass values, and subsequently summed. This method is called the *Superposition-Technique*, and an example of the projected areas are shown in figure 9.9.

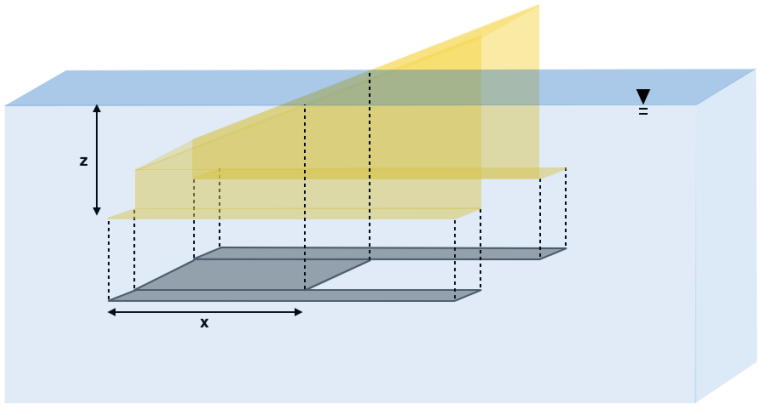

Figure 9.9: Horizontal Lift Through Splash Zone (b) - Superposition-Technique

The other method, the *Plate-Technique*, was based on that the mid-part of the projected area and the flaps up to length x were calculated as *one* area, resulting in *one* added mass value. The rest of the two flaps resulted in *two* added mass values. The total added mass value would be the sum of the three values. An example of this technique is shown in figure 9.10.

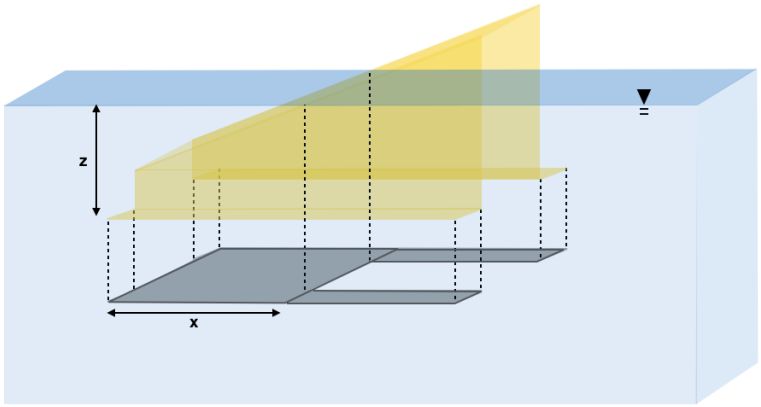

Figure 9.10: Horizontal Lift Through Splash Zone (b) - Plate-Technique

It was assumed that the amount of water trapped inside the immersed cover was identical to the volume of the immersed cover, constrained by the intersection between the sea surface and the cover roof, as shown in figure 9.11.

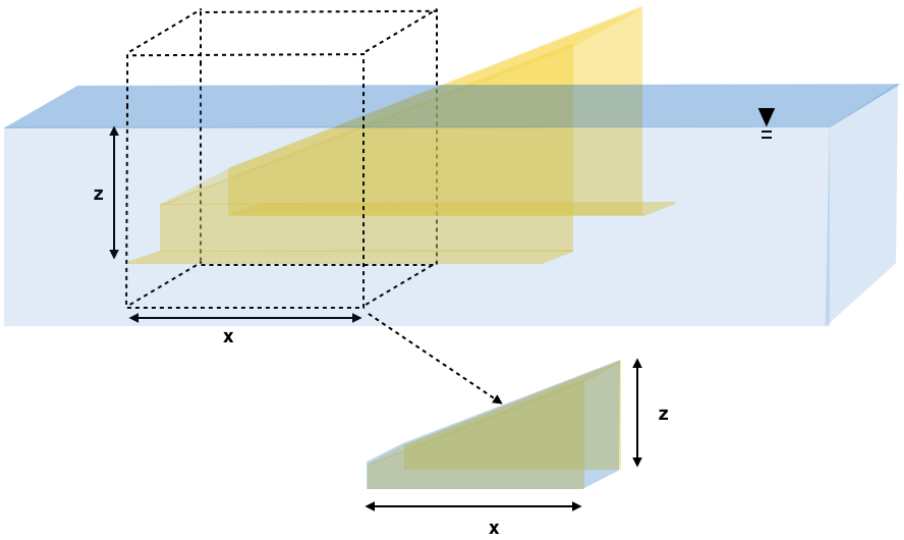

Figure 9.11: Volume of water trapped inside immersed cover

When the cover was half immersed with submerged depth z of 3m, x was 6.5m. The volume of trapped water was 93.1 m^3, resulting in a mass of 95 411 kg.

The added mass value was calculated with the two different techniques and are described in following sections.

Superposition-Technique

Using the Superposition-Technique, the total projected area A_{tot} was two times the area A_1 plus A_2 in figure 9.12. The calculated hydrodynamic parameters are listed in table 9.5.

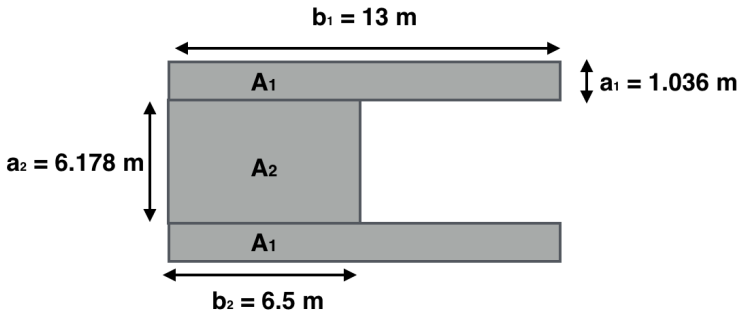

Figure 9.12: Projected area for added mass - Horizontal Lift Through Splash Zone (b), Superposition-Technique

Table 9.5: Hydrodynamic parameters for horizontal lift through splash zone (b) - Superposition-Technique

Parameters	Values for area A_1	Parameters	Values for area A_2
a_1	1.036 m	a_2	6.178 m
b_1	13 m	b_2	6.5 m
$\frac{b_1}{a_1}$	12.548	$\frac{b_2}{a_2}$	1.052
$C_{A,1}$	0.964	$C_{A,2}$	0.592
$V_{R,1}$	10.959 kg	$V_{R,2}$	194.850 kg
$A_{33,1}$	10 828 kg	$A_{33,2}$	118 235 kg
$A_{33,tot}$	**21 656 kg**	**$A_{33,tot}$**	**118 235 kg**

The total added mass value for the immersed cover with a depth of 3m was **235 302 kg**, including the mass of the trapped water.

Plate-Technique

Using the Plate-Technique, the total projected area A_{tot} was two times the area A_1 plus A_2 in figure 9.13. The calculated hydrodynamic parameters are listed in table 9.6.

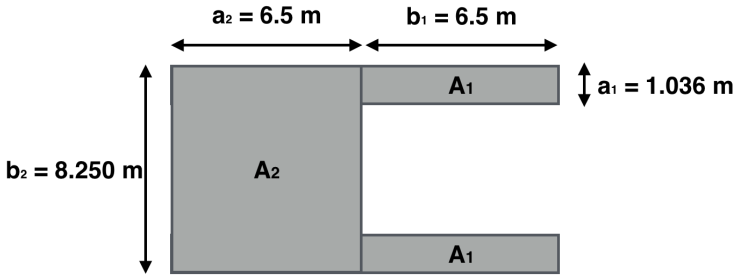

Figure 9.13: Projected area for added mass - Horizontal Lift Through Splash Zone (b), Plate-Technique

Table 9.6: Hydrodynamic parameters for horizontal lift through splash zone (b) - Plate-Technique

Parameters	Values for area A_1	Parameters	Values for area A_2
a_1	1.036 m	a_2	6.500 m
b_1	6.500 m	b_2	8.250 m
$\frac{b_1}{a_1}$	6.274	$\frac{b_2}{a_2}$	1.269
$C_{A,1}$	0.917	$C_{A,2}$	0.646
$V_{R,1}$	5.479 kg	$V_{R,2}$	273.76 kg
$A_{33,1}$	5 150 kg	$A_{33,2}$	181 270 kg
$A_{33,tot}$	**10 300 kg**	**$A_{33,tot}$**	**181 270 kg**

The total added mass value for the immersed cover with a depth of 3m was **286 981 kg**, including the mass of the trapped water.

Drag Force

The projected area used to calculate the drag force is shown in figure 9.14. The total drag force woulb be the sum of the drag forces found by area A_2 and two times the drag force found by area A_1. The parameters used in the calculation of the drag force can be found in table 9.7.

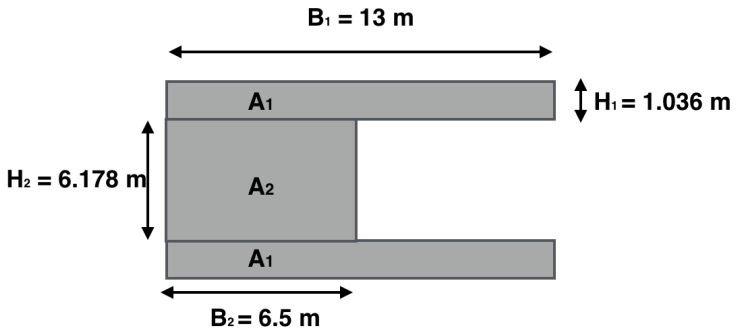

Figure 9.14: Projected area for drag force - Horizontal Lift Through Splash Zone (b)

Table 9.7: Drag force parameters for horizontal lift through splash zone (b) - half immersed

Parameters	**Values for area A_1**	**Parameters**	**Values for area A_2**
B_1	13 m	B_2	6.5 m
H_1	1.036 m	H_2	6.178 m
S_1	13.468 m^2	S_2	40.157 m^2
$\frac{B_1}{H_1}$	12.548	$\frac{B_2}{H_2}$	1.052
$C_{DS,1}$	1.653	$C_{DS,2}$	1.161
v_w	1.91 m/s	v_w	1.91 m/s
v_r	3.00 m/s	v_r	3.00 m/s
$F_{D,1}$	**103 029 N**	**$F_{D,2}$**	**215 763 N**

The total drag force when the cover was half immersed was **421 821 N**.

9.2.1.3 (c) Fully Immersed

The superposition- and plate-technique were used when the added mass value was calculated for the fully immersed cover. The differences in the projected areas are shown in figure 9.15 and 9.16, for the two techniques respectively.

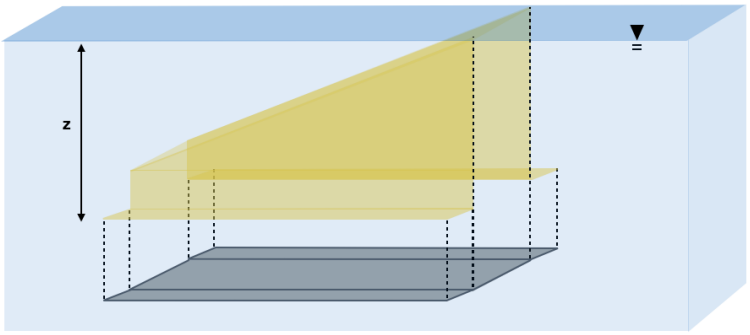

Figure 9.15: Horizontal Lift Through Splash Zone (c) - Superposition-Technique

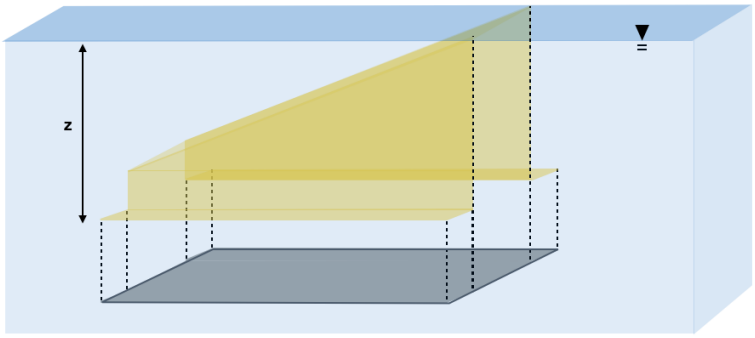

Figure 9.16: Horizontal Lift Through Splash Zone (c) - Plate-Technique

The fully immersed cover, crossing the splash zone, had a submerged depth z of 4.378 m and length x of 13 m. Thus, the volume of trapped water inside the submerged cover was 241.5 m^3, resulting in a mass of 247 542 kg.

Superposition-Technique

Using the Superposition-Technique, the total added mass $A_{33,tot}$ was two times the added mass found by area A_1 plus the added mass found by area A_2 in figure 9.17. The calculated hydrodynamic parameters are listed in table 9.8.

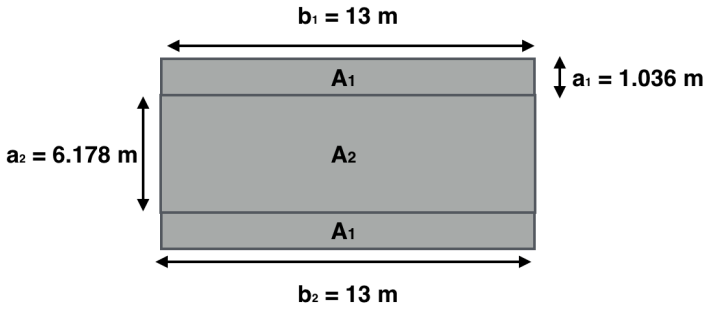

Figure 9.17: Projected area for added mass - Horizontal Lift Through Splash Zone (c), Superposition-technique

Table 9.8: Hydrodynamic parameters for horizontal lift through splash zone (c) - Superposition-Technique

Parameters	**Values for area A_1**	**Parameters**	**Values for area A_2**
a_1	1.036 m	a_2	6.178 m
b_1	13 m	b_2	13 m
$\frac{b_1}{a_1}$	12.548	$\frac{b_2}{a_2}$	2.104
$C_{A,1}$	0.964	$C_{A,2}$	0.766
$V_{R,1}$	10.959 kg	$V_{R,2}$	389.699 kg
$A_{33,1}$	**10 828 kg**	**$A_{33,2}$**	**305 972 kg**

The total added mass value for the immersed cover with a depth of 4.378 m was **575 170 kg**, including the mass of the trapped water.

Plate-Technique

Using the plate-technique, the total added mass $A_{33,tot}$ was the added mass found by area A_1 in figure 9.18. The calculated hydrodynamic parameters are listed in table 9.9.

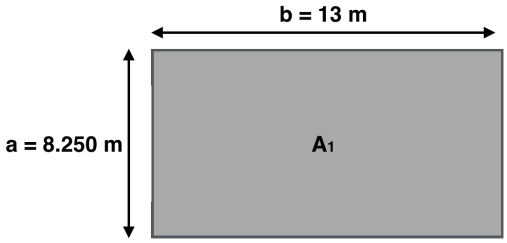

Figure 9.18: Projected area for added mass - Horizontal Lift Through Splash Zone (c), Plate-Technique

Table 9.9: Hydrodynamic parameters for horizontal lift through splash zone (c) - Plate-Technique

Parameters	**Values for area A_1**
a	8.250 m
b	13 m
$\frac{b}{a}$	1.576
C_A	0.702
V_R	694.930 kg
A_{33}	**500 037 kg**

The total added mass value for the immersed cover with a depth of 3 m was **747 579 kg**, including the mass of the trapped water.

Drag Force

The projected area used to calculate the drag force is shown in figure 9.18. The parameters used in the calculation of the drag force are listed in table 9.10.

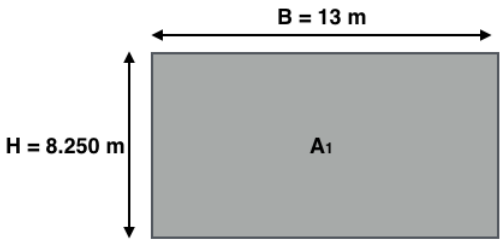

Figure 9.19: Projected area for drag force - Horizontal Lift Through Splash Zone (c)

Table 9.10: Drag force parameters for horizontal lift through splash zone (c) - fully immersed

Parameters	**Values for area A_1**
B	13 m
H	8.250 m
S	107.25 m^2
$\frac{B}{H}$	1.576
C_{DS}	1.166
v_w	1.75 m/s
v_r	2.77 m/s
F_D	**492 111 N**

9.2.2 Fully Submerged

The cover was fully submerged with a depth z of 14.378 m, as shown in figure 9.20. The added mass force was based on the projected area, and was identical to the one found in the *(c) fully immersed phase*; 575 170 kg with the Superposition-Technique and 747 579 kg with the Plate-Technique. The drag force is dependent on the water particle velocity and will vary with depth. The hydrodynamic parameters used to calculate the drag force are listed in table 9.11.

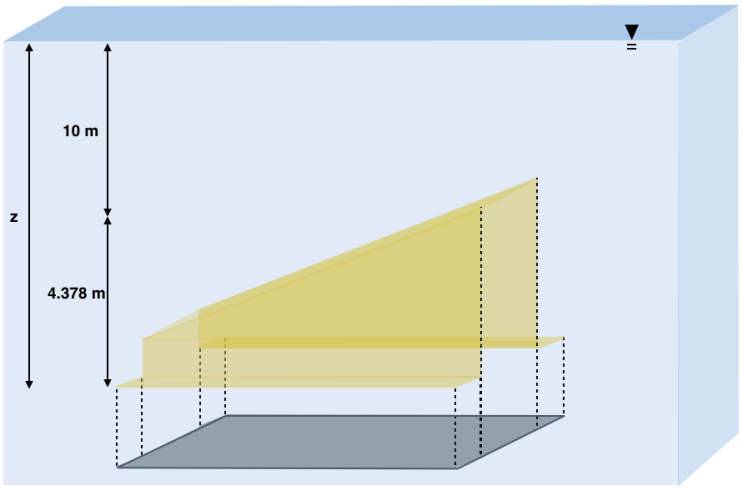

Figure 9.20: Horizontal Lift - Fully Submerged

Table 9.11: Hydrodynamic parameters for horizontal lift - fully submerged

Parameters	**Values for area A_1**
B	13 m
H	8.250 m
S	107.25 m^2
$\frac{B}{H}$	1.576
C_{DS}	1.166
v_w	0.93 m/s
v_r	1.62 m/s
F_D	**167 677 N**

9.3 Summary of Hydrodynamic Parameters

A summary of the hydrodynamic parameters for a lift with vertical- and horizontal rigging are listed in table 9.12 and 9.13 respectively. For added mass, the most conservative values, were found by the Plate-Technique, and are the ones listed below. There will be no hydrodynamic forces acting in *phase 1 - In air*.

Table 9.12: Summary of hydrodynamic parameters during different phases in a vertical lift

Vertical Rigging	**z**	**d**	**A_{33}**	**F_D**
2 - Through Splash Zone				
(a) half immersed	6.500 m	0.609 m	8 300 kg	52 664 N
(b) fully immersed	13.000 m	7.303 m	29 130 kg	49 051 N
3 - Fully Submerged	23.000 m	17.303 m	29 130 kg	17 484 N

Table 9.13: Summary of hydrodynamic parameters during different phases in a horizontal lift

Horizontal Rigging	**z**	**d**	**A_{33}**	**F_D**
2 - Through Splash Zone				
(a) only flaps immersed	1.636 m	0.275 m	21 656 kg	298 984 N
(b) half immersed	3.000 m	1.639 m	286 981 kg	421 821 N
(c) fully immersed	4.378 m	3.081 m	747 579 kg	492 111 N
3 - Fully Submerged	14.378 m	13.081 m	747 579 kg	167 677 N

10 Resulting Force with Simplified Method

The Simplified Method is used to determine the resulting force working on the total system. Not all the specified forces in the Simplified Method will act during the different lifting phases. Table 10.1 shows an overview of which forces that affect the resulting force during the different phases. The inertia force and weight of the cover will be present at all times.

Table 10.1: Overview of significant forces through different lifting phases

	Drag	Slamming	Inertia	Varying Buoyancy	Buoyancy	Mg
Phase 1			√			√
Phase 2	√	√	√	√	√	√
Phase 3	√		√		√	√

When hydrodynamic parameters were calculated, the *Plate-Technique* provided a significantly higher added mass value than the *Superpostition-Technique*. Due to DNV GL's recommendation of not using the superposition technique (DNV GL, 2011b), the most conservative values for the added mass - found by the *Plate-Technique*, are used in further calculation.

Rates of change of added mass with submergence $\frac{dA_{33}^{\infty}}{dh}$ are listed in table 10.2 and 10.3, for vertical and horizontal rigging respectively, and are used to calculate the slamming coefficients.

Table 10.2: Rates of change of added mass with submergence - vertical rigging

Vertical Rigging	$\frac{dA_{33}^{\infty}}{dh}$
Half immersed	1 277 kg/m
Fully immersed	3 205 kg/m

Table 10.3: Rates of change of added mass with submergence - horizontal rigging

Horizontal Rigging	$\frac{dA_{33}^{\infty}}{dh}$
Only flaps immersed	13 237 kg/m
Half immersed	194 520 kg/m
Fully immersed	334 241 kg/m

10.1 Vertical Rigging

10.1.1 In Air

The resulting force for vertical rigging in *phase 1 - In Air* is given by equation 10.1.

$$F_{Res} = F_I + Mg_{air} \tag{10.1}$$

The inertia force F_I was found by equation 10.2.

$$F_I = \sqrt{[(M_{air} + A_{33})\ddot{\eta}_{ct}]^2 + [(\rho V + A_{33})\dot{v}_w]^2} \tag{10.2}$$

In air, the added mass A_{33} and the volume of displaced water V was zero. It was assumed that the crane tip acceleration $\ddot{\eta}_{ct}$ followed the linear wave acceleration in heave $\dot{v}_w$ and was calculated by (8.16). With a submerged depth of zero, $\ddot{\eta}_{ct} = \dot{v}_w$ = 1.67 m/s^2.

The cover mass in air M_{air} was 11 900 kg and had a weight Mg_{air} of 116 739 N. Thus, the inertia force was calculated to be $F_I = \sqrt{[11900 \cdot 1.67]^2}$ = 19 873 N.

The resulting force was calculated by equation (10.1) and is listed in table 10.4 in addition to the other acting forces.

Table 10.4: Resulting Force, Vertical Lift - In Air

Forces	Magnitude
F_I	19 873 N
Mg_{air}	116 739 N
F$_{res}$	**136 612 N**

10.1.2 Through Splash Zone

10.1.2.1 (a) Half Immersed

The resulting force for vertical rigging in *phase 2 - Through Splash Zone* with a half immersed cover is given by equation 10.3.

$$F_{Res} = \sqrt{(F_D + F_S)^2 + (F_I - F_B)^2} + Mg_{air} - F_{buoy} \tag{10.3}$$

The water particle velocity and acceleration v_w and $\dot{v}_w$ are calculated by (8.15) and (8.16) respectively. The cover was half immersed through the splash zone with a submerged depth to COG d of

0.609 m. Thus, v_w = 2.04 m/s and $\dot{\eta}_{ct} = \dot{v}_w$ = 1.60 m/s^2. The water plane area A_w was 0.3 m^2 with a cover thickness of 0.021 m. Submerged volume V was 2.382 m^3.

It was assumed that v_{ct} = v_w, thus the relative velocity between the object and the water particles v_r = $v_c + \sqrt{2v_w^2}$ = 3.19 m/s.

The slamming force F_S was calculated by equation (8.20). The slamming impact velocity v_s was identical to the relative velocity between the cover and the water particles of 3.19 m/s. The slamming area A_S was the projected area of the submerged cover of 8.47 m^2.

The slamming coefficient was calculated by equation (8.21) to be $C_S = \frac{2}{1025 \cdot 8.47} \cdot 1277$ = 0.294, with a rate of change of added mass of 1 277 kg/m. Hence, F_S was 12 987 N and F_I was 36 605 N.

The varying buoyancy force was calculated by equation (8.23) and (8.24). It was assumed that the characteristic single amplitude vertical motion of the crane tip η_{ct} was identical to ζ_a of 2.7 m. Hence, δV was 1.14 m^3 and F_B was 11 489 N.

The buoyancy force F_{buoy} was 23 952 N and is the weight of displaced water.

The resulting force was calculated by equation (10.3) and was listed in table 10.5 in addition to the other acting forces.

Table 10.5: Resulting Force, Vertical Lift - Through Splash Zone, (a) half immersed

Forces	Magnitude
F_D	52 664 N
F_S	12 987 N
F_I	36 605 N
F_B	11 489 N
Mg_{air}	116 739 N
F_{buoy}	23 952 N
F_{res}	**163 078 N**

10.1.2.2 (b) Fully Immersed

The resulting force for vertical rigging in *phase 2 - Through Splash Zone* with a fully immersed cover was given by equation 10.4.

$$F_{Res} = \sqrt{(F_D + F_S)^2 + (F_I - F_B)^2} + Mg_{subm} - F_{buoy} \tag{10.4}$$

The cover was fully immersed through splash zone with a submerged depth to COG d of 7.303 m. Thus, v_w = 1.34 m/s and $\dot{\eta}_{ct} = \dot{v}_w$ = 1.05 m/s^2. The water plane area A_w was 0.357 m^2

and submerged volume V was 4.287 m^3. The relative velocity between the cover and the water particles v_r was 2.20 m/s, which is identical to the slamming velocity v_s. The slamming area A_S is the projected area of submerged cover of 16.94 m^2. Hence, the slamming coefficient C_S was 0.369, with a rate of change of added mass as listed in table 10.2 of 3 205 kg/m. Thereafter, F_S was calculated to be 15 505 N and F_I was 55 633 N.

Varying volume due to oscillation δV was 1.36 m^3, hence F_B was 13 707 N. The buoyancy force F_{buoy} was 43 107 N.

The resulting force was calculated by equation (10.4) and is listed in table 10.6 in addition to the other acting forces.

Table 10.6: Resulting Force, Vertical Lift - Through Splash Zone, (b) fully immersed

Forces	Magnitude
F_D	49 051 N
F_S	15 505 N
F_I	55 633 N
F_B	13 707 N
Mg_{air}	116 739 N
F_{buoy}	43 107 N
F$_{res}$	**150 608 N**

10.1.3 Fully Submerged

The resulting force for vertical rigging in *phase 3 - Fully Submerged* is given by equation 10.5.

$$F_{Res} = \sqrt{F_D^2 + F_I^2} + Mg_{air} - F_{buoy} \tag{10.5}$$

The cover was fully submerged with a submerged depth to COG d of 17.303 m. Thus, $v_w = 0.71$ m/s and $\ddot{\eta}_{ct} = \dot{v}_w$ = 0.56 m/s^2. The relative velocity between the cover and the water particles v_r was 1.31 m/s. The water plane area A$_w$ was zero, resulting in no varying buoyancy nor any slamming force. Submerged volume V was 4.287 m^3, hence F_I was 29 672 N. The buoyancy force will be identical to the one calculated for the *fully submerged through splash zone*-phase.

The resulting force was calculated by equation (10.5) and listed in table 10.7 in addition to the other acting forces.

Table 10.7: Resulting Force, Vertical Lift - Fully Submerged

Forces	Magnitude
F_D	17 484 N
F_I	29 672 N
Mg_{air}	116 739 N
F_{buoy}	43 107 N
F_{res}	**120 788 N**

10.2 Horizontal Rigging

10.2.1 In Air

In air, the resulting force F_{res} will be constant independently on the rigging. Thus, as calculated for vertical rigging, F_I was 19 873 N, Mg_{air} was 116 739 N, and the resulting force was **136 612 N**.

10.2.2 Through Splash Zone

10.2.2.1 (a) Only flaps immersed

The resulting force for horizontal rigging in *phase 2 - Through Splash Zone*, when only the cover flaps are immersed, is given by equation 10.6.

$$F_{Res} = \sqrt{(F_D + F_S)^2 + (F_I - F_B)^2} + Mg_{air} - F_{buoy} \tag{10.6}$$

The water particle velocity and acceleration v_w and $\dot{v}_w$ are calculated by (8.15) and (8.16) respectively. The cover was immersed through the splash zone with a submerged depth to COG d of 0.275 m. Thus, v_w = 2.08 m/s and $\ddot{r}_{ct} = \dot{v}_w$ = 1.64 m/s^2. The water plane area A_w was 0.546 m^2 and the submerged volume V was 2.064 m^3.

It was assumed that $v_{ct} = v_w$. Thus, the relative velocity between the cover and the water particles $v_r = v_c + \sqrt{2v_w^2}$ = 3.24 m/s, which is identical to the slamming velocity v_s. The slamming force F_S was calculated by equation (8.20). The slamming area A_S is the projected area of submerged cover of 26.94 m^2.

The slamming coefficient was calculated by equation (8.21), and with a rate of change of added mass found in table 10.3 of 13 237 kg/m, C_S was 0.959. Hence, F_S was calculated to be 138 957 N and F_I was 67 442 N.

The varying buoyancy force was calculated by equation (8.23) and (8.24). δV was calculated to be 2.08 m^3, hence F_B was 20 964 N. The buoyancy force F_{buoy} was 20 754 N.

The resulting force was calculated by equation (10.6) and listed in table 10.8 in addition to the other acting forces.

Table 10.8: Resulting Force, Horizontal Lift - Through Splash Zone, (a) only flaps immersed

Forces	Magnitude
F_D	298 984 N
F_S	138 957 N
F_I	67 442 N
F_B	20 964 N
Mg_{air}	116 739 N
F_{buoy}	20 754 N
F$_{res}$	**536 385 N**

10.2.2.2 (b) Half Immersed

The resulting force for horizontal rigging in *phase 2 - Through Splash Zone*, when the cover is half immersed, is given by equation 10.7.

$$F_{Res} = \sqrt{(F_D + F_S)^2 + (F_I - F_B)^2} + Mg_{air} - F_{buoy} \tag{10.7}$$

The cover was half immersed in horizontal direction crossing the splash zone, with a submerged depth to COG d of 1.639 m. Thus, v_w = 1.91 m/s and $\ddot{\eta}_{ct} = \dot{v}_w$ = 1.50 m/s^2. The water plane area A_w was 0.403 m^2 and submerged volume V was 3.484 m^3. The relative velocity between the cover and the water particles v_r was 3.00 m/s, and is identical to the slamming velocity v_s.

The slamming area A_S is the projected area of submerged cover of 53.625 m^2. The slamming coefficient C_S was calculated to be 7.078, by use of the rate of change of added mass, found in table 10.3 of 194 520 kg/m. Hence, F_S was 1 750 680 N and F_I was 625 251 N.

Varying volume due to oscillation δV, was calculated to be 1.54 m^3, hence F_B was 15 473 N and the buoyancy force F_{buoy} was 35 032 N.

The resulting force was calculated by equation (10.7) and listed in table 10.9 in addition to the other acting forces.

Table 10.9: Resulting Force, Horizontal Lift - Through Splash Zone, (b) half immersed

Forces	Magnitude
F_D	421 821 N
F_S	1 750 680 N
F_I	625 251 N
F_B	15 473 N
Mg_{air}	116 739 N
F_{buoy}	35 032 N
F$_{res}$	**2 338 162 N**

10.2.2.3 (c) Fully Immersed

The resulting force for horizontal rigging in *phase 2 - Through Splash Zone*, when the cover was fully immersed, is given by equation 10.8.

$$F_{Res} = \sqrt{(F_D + F_S)^2 + (F_I - F_B)^2} + Mg_{air} - F_{buoy} \tag{10.8}$$

The cover was fully immersed in horizontal direction crossing the splash zone, with a submerged depth to COG d of 3.081 m. Thus, v_w = 1.75 m/s and $\ddot{\eta}_{ct} = \dot{v}_w$ = 1.37 m/s^2. The water plane area A_w was 0.130 m^2 and submerged volume V was 4.287 m^3. The relative velocity between the cover and the water particles v_r was 2.77 m/s, identical to the slamming velocity v_s.

The slamming area A_S is the projected area of submerged cover of 107.25 m^2. The slamming coefficient C_S was calculated to be 6.081, by use of the rate of change of added mass, found in table 10.3 of 334 241 kg/m. Hence, F_S was 2 564 598 N and F_I was 1 464 217 N.

Varying volume due to oscillation δV, was calculated to be 0.496 m^3, hence F_B 4 991 N and the buoyancy force F_{buoy} was 43 107 N.

The resulting force was calculated by equation (10.8) and listed in table 10.10 in addition to the other acting forces.

Table 10.10: Resulting Force, Horizontal Lift - Through Splash Zone, (c) fully immersed

Forces	Magnitude
F_D	492 111 N
F_S	2 564 598 N
F_I	1 464 217 N
F_B	4 991 N
Mg_{air}	116 739 N
F_{buoy}	43 107 N
F$_{res}$	**3 460 786 N**

10.2.3 Fully Submerged

The resulting force for horizontal rigging in *phase 3 - Fully Submerged* was given by equation 10.9.

$$F_{Res} = \sqrt{F_D^2 + F_I^2} + Mg_{air} - F_{buoy} \tag{10.9}$$

The cover was fully submerged with a submerged depth to COG d of 13.081 m. Thus, v_w = 0.93 m/s and $\ddot{\eta}_{ct} = \dot{v}_w$ = 0.73 m/s^2. The relative velocity between the cover and the water particles v_r was 1.62 m/s. The water plane area A_w was zero, resulting in no varying buoyancy nor any slamming force. Submerged volume V was 4.287 m^3, hence F_I was 780 203 N. The buoyancy force will be identical to the one calculated in the *fully submerged through splash zone*-phase.

The resulting force was calculated by equation (10.9) and listed in table 10.11 in addition to the other acting forces.

Table 10.11: Resulting Force, Horizontal Lift - Fully Submerged

Forces	Magnitude
F_D	167 677 N
F_I	780 203 N
Mg_{air}	116 739 N
F_{buoy}	43 107 N
F$_{res}$	**871 650 N**

10.3 Summary of Resulting Forces

The resulting forces that arise during the different lifting phases are listed in table 10.12 and 10.13 for vertical and horizontal rigging respectively.

Table 10.12: Summary of Resulting Forces - Vertical Lift

Vertical Lift	F_{res}
1 - In Air	136 612 N
2 - Through Splash Zone	
(a) Half immersed	163 078 N
(b) Fully immersed	150 608 N
3 - Fully Submerged	120 788 N

Table 10.13: Summary of Resulting Forces - Horizontal Lift

Horizontal Lift	F_{res}
1 - In Air	136 612 N
2 - Through Splash Zone	
(a) Only flaps immersed	536 385 N
(b) Half immersed	2 338 162 N
(c) Fully immersed	3 460 786 N
3 - Fully Submerged	871 650 N

10.4 Oscillation Period

Resonance in a system should be avoided at any time. Resonance is a phenomenon where an external force drives another system to oscillate with larger amplitude, and will arise when the natural period of the system T_N is equal to the zero-crossing period T_z.

Equation (8.9) was used to find the equation for the natural period of the system as shown in figure (10.10), where the hoisting line stiffness k equals $\frac{EA}{L}$.

$$T_N = 2\pi\sqrt{\frac{M + A_{33}}{k}} \tag{10.10}$$

T_z was determined to be 8 seconds, thus resonance will occur if T_N approaches 8 s. To avoid resonance during the different lifting phases with varied submerged depth and length of lifting wire L, $EA_{critical}$ (10.11) was found, and are listed in table 10.14 and 10.15, for vertical and horizontal rigging respectively. The crane tip was located 30 m above sea surface

$$EA_{critical} = \frac{4\pi^2}{8^2} \cdot (M + A_{33}) \cdot L \tag{10.11}$$

Table 10.14: System Natural Period - Vertical Lift

Vertical Lift	A_{33}	L	$EA_{critical}$
2 - Through Splash Zone			
(a) Half immersed	8 300 kg	23.5 m	293 kN
(b) Fully immersed	29 130 kg	30 m	759 kN
3 - Fully Submerged	29 130 kg	40 m	1 012 kN
4 - Landing			
at Heidrun	29 130 kg	350 m	8 858 kN
at Tanzania	29 130 kg	2460 m	62 261 kN

Table 10.15: System Natural Period - Horizontal Lift

Horizontal Lift	A_{33}	L	$EA_{critical}$
2 - Through Splash Zone			
(a) Only flaps immersed	21 656 kg	27 m	559 kN
(b) Half immersed	286 981 kg	30 m	5 531 kN
(c) Fully immersed	747 579 kg	31 m	14 523 kN
3 - Fully Submerged	747 579 kg	51 m	23 893 kN
4 - Landing			
at Heidrun	747 579 kg	350 m	163 979 kN
at Tanzania	747 579 kg	2460 m	1 152 473 kN

10.5 Limited Resulting Force

In aforementioned sections the crane tip velocity $\dot{\eta}_{ct}$ was assumed to be identical to the water particle acceleration. Hence, maximum resulting forces was yielded. The calculations in this section in based upon the assumption that the crane tip velocity is zero. The drag forces are dependent on the crane tip velocity, and the calculated drag forces are listed in table 10.16 and 10.17 in addition to the new limited resulting forces that arise during the different lifting phases, for vertical and horizontal rigging respectively. No drag forces are acting during the in-air phase, thus the resulting force will not be changed by introducing the new assumption.

Table 10.16: Limited Resulting Force - Vertical Lift

Vertical Rigging	v_w	v_r	F_D	$\mathbf{F}_{res}$	**Deviation**
2 - Through Splash Zone					
(a) Half immersed	2.04 m/s	2.34 m/s	28 409 N	141 206 N	13%
(b) Fully immersed	1.34 m/s	1.64 m/s	27 382 N	133 608 N	11%
3 - Fully Submerged	0.71 m/s	1.01 m/s	10 393 N	105 071 N	13%

Table 10.17: Limited Resulting Force - Horizontal Lift

Horizontal Rigging	v_w	v_r	F_D	$\mathbf{F}_{res}$	**Deviation**
2 - Through Splash Zone					
(a) Only flaps immersed	2.08 m/s	2.38 m/s	160 535 N	399 062 N	26%
(b) Half immersed	1.91 m/s	2.21 m/s	228 913 N	2 153 088 N	8%
(c) Fully immersed	1.75 m/s	2.05 m/s	269 533 N	3 261 365 N	6%
3 - Fully Submerged	0.93 m/s	1.23 m/s	96 662 N	859 800	1%

11 Discussion

The α-factor is based on few locations, but used to plan operations world wide. The wave conditions at Heidrun and Tanzania are highly different. The waves that arise outside Tanzania are rarely higher than 3 m, and the ones that arise outside Heidrun are significantly higher. Nevertheless the same α-factor is used. Even though the waves do not exceed 3 m, there is a significant difference in the operability when Hs_{LIM} is 2 m and 3 m, especially during winter. By using a local α-factor instead of those gathered from the North Sea, more adequate operational criteria might be achieved and increase the operation operability. At Heidrun it will be of high importance trying to increase the operational criteria, but at Tanzania this will we pointless for OP_{WF} larger than 3 m. The water depth outside Tanzania is significantly deeper than at Heidrun, and strong currents arise here. The operational criteria should instead of, or in addition to, being based on an α-factor for waves, be based on an α-factor for currents.

Weather forecasts are based on *one* parameter, significant wave height Hs, and sometimes the peak period Tp. Only vertical forces and motions are investigated, which is an accurate but not exact assumption. During the actual operation it is up to the Captain and the Deck Foreman to decide whether the environmental conditions are within the criteria, in such a way that the operation can take place safely or not. This decision is based upon practical experience and the real motions of the vessel. In some cases this decision results in a lower operational criteria than planned. A way of avoiding this can be by plan the operational criteria based on the the actual response that will arise in the system.

The α-factor has not been revised since 2006, for many reasons because this will be a expensive and long process. The industry has to be willing to invest in such a process, and for them to accept this, the return of the investment has to be positive. The changes in the α-factors have to result in increased operational limits, in order to extend the season where installation activities can be performed and reduce the time for waiting-on-weather, in the order of getting an economic benefit.

When the cover is installed horizontally there are at least two ways of determining the added mass value. One of the techniques give a significantly higher value than the other one. Added mass for more complex three-dimensional structures compared to the ones listed in DNV GL's rules and standards, should be determined by experiments. It is a reason to believe that there is coupling effects in added mass making superposition of the projected area not recommended.

The added mass is highly dependent on the projected area of the submerged part of the cover. Lifting the cover in such a way that the projected area is minimised, will most likely be the most efficient way to perform the operation, in terms of acting forces and operability. Minimised projected area will most likely occur when the cover is lifted in vertical direction with a tilt of 13°, which is the angle of the inclined cover roof. Thus, the cover roof will, instead of the cover flaps, be 90° to the sea surface and not contribute to the projected area. The two flaps will independently contribute to

the projected area and the added mass will most likely be significantly smaller.

Due to the inclined cover roof the assumption about estimating the added mass based on the projected area of the submerged part, as a thin plate, will most likely be underestimate the total added mass value. No estimations of inclined plates are given in any rules or standards, thus this kind of estimation should be simulated using e.g. WAMIT.

Due to the ratio between the light weight of the cover in air and the large added mass and drag forces when the cover is submerged, strict operational criteria are given for the operation. A GRP cover is a less complicated structure made of cheap material and is usually installed during another subsea installation. A dilemma may arise where one has to determine whether one should wait on weather, which is highly expensive due to the offshore day-rates, or take a chance and install the cover outside the weather window. A GRP cover replacement may be cheaper than the costs of waiting on weather.

The hoisting line's $EA_{critical}$ has a large range for especially for the deep water operation at Tanzania. If the EA-criteria cannot be met by chosen lifting equipment, resonance will occur and use of heave compensation should be discussed.

When the crane tip velocity $\dot{\eta}_{ct}$ was assumed to be zero, relative to the wave particle velocity v_w, the resulting force for vertical rigging deviated with approximately 13% from the resulting force found for $\dot{\eta}_{ct} = v_w$. For horizontal rigging the resulting force deviated with 26% when only the flaps were immersed and less than 8% during further lowering. When the cover was installed in horizontal direction the slamming load and inertia force were dominating. The drag force would therefore be of no significant importance. There is evidence to believe that the estimated resulting force found for *worst-case scenario*, when $\dot{\eta}_{ct} = v_w$, is an adequate estimate.

11.1 Error Sources

Errors will always be present when working with a model. It is not possible to make a perfect model of a real system and some of the assumptions that are introduced will result in modelling errors. However, if the assumptions are adequate and reliable, these errors will be limited.

Average operability is found on season basis, and because of leap years small deviations will be present in the operation operability and downtime.

Wind and current have not been included in the operation planning process. For light structures wind can limit the operational criteria in the *In air*-phase, and current can result in large offset which will increase T_{POP} due to relocation of the cover.

For simplicity the calculations are based on linear wave theory and regular waves. Real waves are irregular and non-liner, but calculations based on this theory is difficult and time-consuming, and

should be considered when the operation is simulated.

The added mass is calculated based on many assumptions. Surface effects and the cover wall's affect are neglected. Water trapped inside the cover will not necessarily fill the whole submerged volume. These assumptions introduce errors that will follow in the calculation of the resultant forces. Added mass- and drag coefficients are well known for two-dimensional and three-dimensional compact bodies of simple geometry. They are adequately well understood for two-dimensional porous plates, but not for three-dimensional complex structures. The drag coefficients given by DNV GL are valid for a steady current, and corrections must be made for oscillatory flow.

12 Conclusion

12.1 Operability

At Heidrun there is significant season variation in terms of operability. Lower significant wave height will arise during summer compared to winter. Thus, operations with strict operation criteria should take place during summer season. An increase of the operational criteria can result in an extension of the season where the installation can be performed. At Tanzania this is not entirely the case. There are small differences in season operability, except from the winter season. Despite this, there are large differences between the operability for a design criterion of 2 m and 3 m. For such an increase in the design criterion Hs_{LIM}, the operability at Heidrun and Tanzania increases with approximately 25 %. The operability at Tanzania converges towards 100 % with Hs_{LIM} om 3 m, and further increase of Hs_{LIM} will make no difference here. At Heidrun further increase of Hs_{LIM} will continue to increase the operability.

The time of waiting-on-weather is due to both storm periods and calm periods of shorter duration than the reference period $Calm - Wait$. Both at Heidrun and Tanzania the contribution from $Calm - Wait$ is minimal.

The length of calms are considerably longer at Tanzania than at Heidrun. For an operation with Hs_{LIM} of 3 m, the mean length of calms at Tanzania varies between 844 hours during winter and 14 594 hours during summer. At Heidrun the mean length of calm varies between 46 hours during winter and 207 hours during winter.

The length of calms at both Heidrun and Tanzania fit a Weibull distribution pretty good. At Heidrun the shape parameter β is just above 1 and the distribution will be similar to an exponential distribution. In terms of reliability the failure rate will increase. The scale parameter γ varies between 37 and 203. A large scale parameter at constant β will stretch out the probability density function which indicates that the data set are widely spread. At Tanzania β is just below 1, and the distribution will also be close to an exponential distribution. The failure rate decreases in terms of reliability. γ has an enormous range and varies between 72 and 14 957. Therefore, there are strong evidence to believe that the length of calms at Tanzania are fairly more spread out than at Heidrun.

12.2 Resulting Forces

A vertical rigging of the pipeline GRP cover will result in a significantly lower maximum resultant force than a lift with horizontal rigging. Therefore, it will be recommended to use a vertical form of rigging when installing the cover.

For horizontal rigging the slamming force dominates while crossing the splash zone. Regardless

of how the cover is lifted significantly larger forces act on the system during this phase. Due to decreased vertical velocity with submerged depth, the forces in heave direction will diminish for further lowering.

The Superposition-Technique and Plate-Technique used to calculate the added mass value with different projected areas, result in large differences in calculated value. Superposition is not recommended due to a non-linear relationship between the added mass value and the projected area. Despite this superposition is used as a part of the Plate-Technique e.g. through splash zone, when the cover is half immersed. It is hard to tell which method that yields correct result, and the results should be compared with results from model tests.

In worst-case scenario, when the crane tip acceleration is identical to the wave particle acceleration, the maximum resulting forces for horizontal- and vertical rigging are approximately 160 kN and 3 500 kN respectively. If the crane tip acceleration is assumed static, the maximum resulting forces for horizontal- and vertical rigging are approximately 141 kN and 3 261 kN respectively.

The stiffness in the lifting wire will decreases with length, and will result in decreased oscillation frequency and increased oscillation period.

For a vertical lift with T_z of 8 s, resonance will arise during the lift if the hoisting line's EA is between 0.3 MN and 8.9 MN at Heidrun, and 300 kN and 62 000 kN at Tanzania. For a horizontal lift, resonance will arise during the lift if EA is between 0.6 MN and 164 MN at Heidrun and 0.6 MN and 1 152 MN at Tanzania.

12.3 Recommendations for Further Work

A vertical and horizontal lift of the cover are two lifting extremes investigated in this paper. Two be able to find the optimal and most efficient way to perform the lift, different lifting angles should be investigated and simulated. Advantages or disadvantages of using light module handling systems or other methods to transfer the cover through the splash zone should be examined in terms of efficiency and cost.

To be able to determine which added mass-technique that is most appropriate, the estimated hydrodynamic parameters should be compared to model test results of the pipeline GRP cover. Simulation of the installation operation should be performed in SIMO with desired rigging and hydrodynamic parameters. WAMIT can be used to determine exact added mass for the cover with inclined roof.

After adequate hydrodynamic parameters are determined, new methods of installing the covers should be investigated. Perhaps more than one cover can be installed at the same time, or maybe installation of the cover with high operational criteria will be more cost effective than waiting on weather.

Before the operation can take place capacity checks have to be performed on the crane, rigging equipment and structure.

References

Alvær, P. (2008). DNV α-Factor. *KTF - Subsea Lifting Operations, Stavanger 2008 - 03.12.2008*.

Brandsvoll, R. A. (2016). The Different Phases of a Subsea Lift. *Subsea 7 presentation at Subsea Lifting Operations Seminar, Stavanger - 06.12.2016*.

Bøe, T. (2016). Estimation of Hydrodynamic Forces during Subsea Lifting. *DNV GL Oil & Gas - Presentation at Subsea Lifting Operations Seminar, Stavanger - 06.12.2016*.

DNV (2007). Marine Operations Rules, Revised Alpha Factor - Joint Industry Project. Technical Report 2006_1756, DNV. Rev 3, 27.06.2007.

DNV GL (2008). Offshore Standard - Design of offshore steel structures, general (LRFD method). *DNV-OS-C101*.

DNV GL (2011a). Offshore Standard - Marine Operations - General. *DNV-OS-H101*.

DNV GL (2011b). Recommended Practice - Modelling and Analysis of Marine Operations. *DNV-RP-H103*.

DNV GL (2014). Offshore Standard - Lifting Operations (VMO Standard - Part 2-5). *DNV-OS-H205*.

Eik, K. J. and Nygaard, E. (2004). Heidrun - Metocen Design Basis. Technical Report PTT-NKG-RA 0058, Statoil.

Faltinsen, O. M. (1990). *Sea Loads On Ships and Offshore Structures*. Cambridge Ocean Technology. Cambridge University Press.

Gjersvik, T. B. (2015). TPG4200 Subsea Pproduction Systems - NTNU. *Lecture notes*.

Kendon, T. E. (2016). Determination of mass matrix for the GRP cover. Technical report, Statoil. 24.10.2016.

Langen, I. and Sibjörnsson, R. (2009). *Dynamic analysis of structures*. NTNU - Faculty of Engineering Science and Technology.

Larsen, K. (2016). TMR4225 Marine Operations - NTNU. *Lecture Notes*.

Lundby (2006). DNV Marine Operations Revised Alpha Factors. *Presentation - Kranteknisk forening 23.11.2006*.

Mathiesen, M. (2010). Tanzania Block 2 - Metocen Design Basis. Technical Report Metocaen RE-2010-006, Statoil and Polytec Foundation.

Natskår, A., Moan, T., and Alvær, P. (2015). Uncertainty in forecasted environmental conditions for reliability analyses of marine operations. *Ocean Engineering 108 (2015) 636-647*.

Nilsen, F. G. (2016). Installation of Sub-Sea Structures - Estimation of Hydrodynamic Forces. Technical report, Norsk Hydro O&E. Research Centre, Bergen, Field Development. 27.12.02.

NTIS (1973). Snap loads in lifting and mooring cable systems induced by surface wave conditions. Technical Report AD-772 515, Naval Civil Engineering Laboratories. Distributed by National Technical Information Service (NTIS), U.S Department of Commerce, September 1973.

Rahman, M. and Bhatta, D. D. (1993). Evaluation of added mass and damping coefficient of an oscillating circular cylinder. *Applied Mathematical Modelling*, 17:70–79.

ReliaWiki (2016). *The Weibull Distribution*. http://reliawiki.org/index.php/The_Weibull_Distribution. [Accessed 11 December 2016].

Statoil (2015). Aasta Hansteen Subsea Lines and Marine Operations. Technical Report C134-FN-V-KA-0110_02, Statoil. Rev 2, 17.04.2015.

Tharigoupla, V. (2016). E-mail correspondence "Aasta Hansteen marine operations - GRP cover installation. E-mail from VETH@statoil.com to erlmy@statoil.com. Received 08.09.2016 08:49.

TSI (2016). *Wave Energy and Wave Changes with Depth*. Exploring our fluid earth, Teaching Science as Inquiry (TSI) http://reliawiki.org/index.php/The_Weibull_Distribution. [Accessed 13 December 2016].

van Voorthuysen, E. (2015). MANF4430 Reliability and Maintenance Engineering - UNSW. *Lecture notes*.

A Appendices

A.1 α-factor for Waves

Table A.1: α-factor for waves, level B highest forecast (DNV GL, 2011a)

Operational Period	**Design Wave Height** [m]				
[Hours]	$H_S = 1$	$H_S = 2$	$H_S = 3$	$H_S = 4$	$H_S = 6$
$T_{POP} \leq 12$	0.68	0.80	0.82	0.83	0.84
$T_{POP} \leq 24$	0.66	0.77	0.79	0.80	0.82
$T_{POP} \leq 36$	0.65	0.75	0.76	0.77	0.80
$T_{POP} \leq 48$	0.63	0.71	0.73	0.75	0.78
$T_{POP} \leq 72$	0.58	0.66	0.69	0.71	0.76

Table A.2: α-factor for waves, level A with meteorologist at site (DNV GL, 2011a)

Operational Period	**Design Wave Height** [m]			
[Hours]	$H_S = 1$	$H_S = 2$	$H_S = 4$	$H_S = 6$
$T_{POP} \leq 12$	0.72	0.84	0.87	0.88
$T_{POP} \leq 24$	0.69	0.80	0.84	0.86
$T_{POP} \leq 36$	0.68	0.78	0.80	0.84
$T_{POP} \leq 48$	0.66	0.75	0.78	0.81
$T_{POP} \leq 72$	0.61	0.69	0.75	0.79

Table A.3: α-factor for waves, monitoring & level A with meteorologist (DNV GL, 2011a)

Operational Period	**Design Wave Height** [m]			
[Hours]	$H_S = 1$	$H_S = 2$	$H_S = 4$	$H_S = 6$
$T_{POP} \leq 4$	0.72	0.84	0.87	0.88
$T_{POP} \leq 12$	0.69	0.80	0.84	0.86
$T_{POP} \leq 24$	0.68	0.78	0.80	0.84
$T_{POP} > 24$	0.66	0.75	0.78	0.81